STATISTICAL ANALYSIS OF MICROGRAVITY TWO-PHASE SLUG FLOW VIA THE DRIFT FLUX MODEL

A Thesis

by

BENJAMIN ANDREW LARSEN

Submitted to the Office of Graduate and Professional Studies of
Texas A&M University
in partial fulfillment of the requirements for the degree of

MASTER OF SCIENCE

Chair of Committee,	Karen Vierow
Committee Members,	Yassin A. Hassan
	Richard Kurwitz
Head of Department,	Yassin A. Hassan

May 2014

Major Subject: Nuclear Engineering

ABSTRACT

The current knowledge of flow parameters for terrestrial two-phase flow was developed through experiments that collected hundreds to thousands of data points. However, the cost associated with microgravity testing make collecting such amounts of microgravity two-phase flow data difficult. Multiple researchers have postulated the microgravity drift flux model parameters to predict void fraction, however, these methods were initially developed with no consideration given to a microgravity environment. The purpose of this thesis was to develop a process by which results from multiple microgravity experiments can be compared on a similar medium and used to develop a larger viable data set than what was previously available and to reliably calculate a value for the void fraction from the available data.

Development of multiphase systems for microgravity requires accurate prediction methods. Utilizing data from multiple microgravity two-phase flow experiments, a statistically consistent slug flow database has been created. The data from 13 different microgravity two-phase flow experiments was vetted using a combination of parametric and non-parametric statistical tests to develop a valid model for the drift flux parameters that meet the axioms of a linear model. The result was a statistically consistent microgravity slug flow data base consisting of 220 data points from 8 different experiments and the associated values for the concentration parameter, C_o, and drift velocity, u_{gj}. A key component for this model was redefining the assumptions in the drift flux model to accurately represent microgravity conditions in calculating the

drift flux parameters. The resultant drift flux parameters are a distribution parameter, C_o = 1.336 ± 0.013 and a drift velocity, u_{gj} = -0.126 ± 0.020.

ACKNOWLEDGEMENTS

I would like to thank Karen Vierow for her help and guidance in completing this work. I would also like to express my sincerest gratitude to Frederick Best, my original advisor and committee chairman, for allowing me the opportunity to work as an undergraduate and graduate researcher for the Interphase Transport Phenomena Laboratory at Texas A&M University and all of the guidance he provided to help shape me into the engineer I have become. Thank you as well to Yassin Hassan for agreeing to be a member of my committee. I would also like to thank Cable Kurwitz for his guidance, help, and patience during my research as well as serving as a member of my committee. Special thanks to Ryoji Oinuma and all the members of the ITP for their assistance in my research as well as all of their hard work on the multitude of physical experiments we fabricated and operated. Special thanks also go to all of the researchers who generously made their data available to me and willingly took the time to converse about their work. Finally I would like to thank my parents Donald and Christine Larsen for their love and support in completing my graduate work.

NOMENCLATURE

Symbol	Description
α	Void Fraction (dimensionless)
$\langle\alpha\rangle$	Average Void Fraction (dimensionless)
α_c	Centerline Void Fraction (dimensionless)
α_w	Wall Void Fraction (dimensionless)
A	Cross Sectional Area (m^2)
C_o	Bubble Distribution Parameter (dimensionless)
D	Pipe Diameter (m)
g	Gravitational Acceleration (m/s^2)
j	Total Volumetric Flux (m/s)
j_v	Gas Volumetric Flux (m/s)
j_l	Liquid Volumetric Flux (m/s)
j_{gj}	Drift-Flux (m/s)
$\langle j\rangle$	Total Superficial Velocity (m/s)
$\langle j_v\rangle$	Gas Superficial Velocity (m/s)
$\langle j_l\rangle$	Liquid Superficial Velocity (m/s)
P	Pressure (N/m^2)
Q_v	Volumetric Gas Flow Rate (m^3/s)
Q_l	Volumetric Liquid Flow Rate (m^3/s)
R	Pipe Radius (m)
r	Radial Variable (m)

r^*	r/R Dimensionless Radial Variable
u_∞	Terminal Velocity (m/s)
u_v	Gas Velocity (m/s)
u_l	Liquid Velocity (m/s)
u_r	Relative Velocity (m/s)
u_{gj}	Void-Fraction Weighted Mean Drift Velocity (m/s)
ρ_v	Density Gas (kg/m^3)
ρ_l	Density Liquid (kg/m^3)
μ_v	Viscosity Gas (N s/m^2)
μ_l	Viscosity Liquid (N s/m^2)
σ	Surface Tension (N/m)

Subscripts and Exponents

c	Subscript denoting centerline
l	Subscript denoting liquid phase
m	Exponent denoting Velocity Distribution
n	Exponent denoting Void Distribution
w	Subscript denoting wall
v	Subscript denoting low density gas or vapor phase

TABLE OF CONTENTS

Page

LIST OF FIGURES

Page

LIST OF TABLES

Page

CHAPTER I

INTRODUCTION AND LITERATURE REVIEW

1.1 INTRODUCTION

The numerous advantages of two-phase flow systems are well established in the everyday terrestrial setting. The thermal transport advantage of two-phase systems over single-phase systems is evident in its range of uses from heating buildings and homes to generating electricity in power plants. The fact that two-phase systems carry more energy per unit mass and require less pumping power per unit mass means that systems can be engineered physically smaller and still produce the same output with lower energy requirements. The realization of compact, low energy cost, high power rating thermal transport two-phase flow loops for reduced gravity applications would allow for more compact thermal management systems. One obstacle in analyzing microgravity two-phase flow is the lack of models for predicting two-phase phenomena, such as void fraction. Another is the difficulty of taking data in microgravity environments, this means that data from experiments is limited and there is a large potential for experimental error. One trend that stands out amongst the literature is that each researcher uses only their data. Thus, conclusions drawn from results will include the individual experimental biases. An approach that utilizes all of the existing data would be more robust and with a greater multitude of data points potentially lends itself to more accurate results. The purpose of this thesis was to develop a process by which results from multiple microgravity experiments can be compared on a similar medium and used

to develop a larger viable data set than previously available and to reliably calculate a value for the void fraction from available data.

The drift-flux model can be used for all flow regimes; however, this thesis research is focused on microgravity slug flow. For slug flow, most of the work has been carried out in terrestrial gravity; very little work has been done with regards to two-phase flow modelling in microgravity conditions. No microgravity data was used in the development of the accepted models from Nicklin, Wilkes, and Davidson (1962) and Zuber and Findlay (1965) for predicting void fraction. The Interphase Transport Phenomena (ITP) group at Texas A&M University has attempted to develop accurate models by conducting multiple two-phase flow microgravity experiments over the past eighteen years, such as those from Reinarts (1993), Chang (1997) Braisted (2004), Valota (2004) and Shephard (2009). The goal of this work is to develop accurate slug parameters for the drift flux model using reduced gravity data collected by the ITP as well as data publicly available from other researchers. The approach is to utilize the drift flux model shown in Equation 1 with a statistically consistent method for determining the slope, C_o, and intercept, u_{gj}.

$$u_g = C_o j + u_{gj} \tag{1}$$

Equation 1 is a linear representation of the actual velocity of the gas, u_g, to the volumetric flux of the two-phase mixture, j, from Collier (2001). The slope represents the bubble distribution across the flow channel while the intercept represents the drift velocity through the flow channel.

Knowing the drift velocity and the bubble distribution parameter one can solve for the void fraction which is the ratio of the gas cross sectional area to the total flow channel area. The actual velocity of the gas is equal to the superficial velocity of the gas divided by the void fraction in Equation 2. The gas superficial velocity, j_v, and the mixture velocity, j, can then be calculated because they are a function of the liquid and gas flow rates which are collected through experimentation. Being able to predict the void fraction as a function of the operating parameters and thermodynamic properties of the working fluids is of great importance to the space and nuclear industries in calculating the true density of a mixture.

$$\frac{j_v}{\alpha} = C_o j + u_{gj} \qquad (2)$$

The bubble distribution parameter corrects the one dimensional homogenous theory, adjusting it to factor in the independent variance of the concentration and velocity profiles across the flow channel. The changes in the profile come from the two-phase nature of the flow and the fact that the liquid and gas can have different velocities leading to the phases being distributed in a non-uniform configuration. Mathematically the drift flux is represented by the average of the product of the flux and concentration over the product of the averages. The local drift velocity is indicative of the local velocity of a fluid particle with respect to the local volumetric flux density of the mixture. If one assumes that the drift velocity is unaffected by the presence of other particles, the drift velocity is equal to the terminal velocity of the particle rising in an infinite medium. This is known as two-phase co-current vertical upflow and is the starting point for understanding two-phase flow in microgravity. Two-phase vertical

upflow is used over horizontal two-phase co-current flow because gravity acts to stratify the liquid to the bottom of the tube and the gas to the top in horizontal co-current flow. In microgravity, this stratification does not occur due to the lack of buoyancy forces acting on the liquid, and thus microgravity two-phase flow regimes resemble the visible characteristics of two-phase vertical upflow. Both Dumitrescu (1943) and Davies and Taylor (1950) experimentally determined the rise velocity of bubbles for two-phase vertical upflow by ignoring the frictional and capillary effects of the force balance and considering only the potential and kinetic energy of the liquid falling around the bubble. That the model was developed without regard to microgravity conditions results in many improper assumptions. These assumptions come from a misunderstanding or improper application of the drift flux model which requires the use of new assumptions specifically for microgravity applications.

1.2 LITERATURE REVIEW

Several researchers have approached the determination of the bubble distribution parameter and drift-velocity. Dumitrescu (1943) and Davies and Taylor (1950) studied the rate of rise of large bubbles through tubes. Their theories and experiments determined the equation for the rise velocity of a bubble through a vertical tube which is incorporated into the drift flux model for two-phase vertical upflow. The Davies and Taylor (1950) experiment consisted of pivoting an inverted beaker containing air so that the air could be released in a stream of bubbles into a tube filled with nitrobenzene. It was found that by adjusting the rate of tilting, it was possible to arrange for the air to be spilled into the tube as a single bubble. The rise velocity determined from these two

experiments is the origin of the coefficient 0.351 in the drift velocity equation discussed in chapter 2. This was an empirical fit to the force balance equation to match the terrestrial two-phase flow data collected. Nicklin, Wilkes, and Davidson (1962) performed a study of long bubbles in vertical tubes which showed that the bubbles rise relative to the liquid ahead of them at a velocity exactly equal to the rise velocity proposed by Dumitrescu and Davies and Taylor. They also derived an expression for determining voidage (sic void fraction) in steady two-phase flow. This expression marks the first time the drift flux equation appears with the coefficient 1.2 for the slope and the drift velocity for the intercept.

Zuber and Findlay (1965) presented a paper on the average volumetric concentration of various two-phase flows by the drift-flux model. Their predictions are compared over multiple two-phase flow regimes and flow parameters including different kinds of working fluids (air-water, water-steam) for vertical up flow. Their conclusions include a statement that the general drift flux expressions are applicable to any flow regime. Therefore, changes in flow regimes alter the values of the drift-velocity and distribution parameter, and other models involving two-phase flow must also take into consideration the flow regime. These models are useful in predicting the average void fraction in a channel and for interpreting results from experiments. Zuber also states that the drift-velocity is dependent upon the momentum transfer between the two phases in the flow, the stress fields in both fluids, and also surface effects at the interface between the two phases. The paper gives a detailed method to calculate the distribution parameter based on the exponents of the flow and concentration profiles. A

corresponding plot based on those exponents shows different values for distribution parameter based on the determined exponent value and bubble shape.

França and Lahey (1992) published a paper on the horizontal flow analysis of the drift-flux in two-phase flow. This experiment showed that a higher value of the bubble distribution parameter and a negative value for the drift velocity were possible due to the displacement experienced by the gas bubble, its expansion due to a higher pressure drop, and the liquid velocity distribution in the slug. The liquid velocity profile in horizontal slug flow was measured by Kvernvold et al. (1984). Kvernvold's experiments led to the development of a translational speed value for the slugs which is directly proportional to the mixture velocity and had a value of 1.52. Kvernvold also showed that changes in the flow rates were reflected in the Taylor bubble and liquid film length, not in the liquid slug length.

The work done by these researchers in the development of the drift flux model has been published in multiple journal and scientific articles as well as text books. Wallis (1969) and Collier (2001) are examples of graduate level text books that site these authors in the development of the terrestrial drift-flux model. However these works do not include data from a microgravity environment in the development of the model.

Dukler et al. (1988) published a paper on the study of gas-liquid flow in reduced gravity. Experiments were performed on the Lewis 100 ft drop tower and the Lewis Learjet. The data consisted of the temperatures, flow rates, pressure drop, and 400 frames/s video. The drop tower only provided 2.2 s of microgravity, while the Lear jet

allowed for 12-22 s of data acquisition depending on the parabola. The drop tower loop test section was a transparent tube 9.52 mm in diameter and 0.457 m long. Air was injected into the liquid through four peripheral holes and the flow was controlled using a calibrated valve. A voltage controlled centrifugal pump controlled the liquid flow rate. It should be noted that the experiment did not use flow meters as rates would not change during drops. The Learjet test loop was designed to fix many of the limitations encountered from the drop tower. Two separate high and low flow rate orifices were used to measure air flow and the liquid flow rate was measured with a turbine meter. The tube diameter was increased to 12.7 mm and the test length to 1.06 m. The recording frame rate stayed a constant 400 frames/s however the frame included an LED display that indicated time in 0.01 s intervals to obtain velocities and sizes of slugs and bubbles. The measured value for the distribution parameter (calculated by bubble velocity divided by total superficial velocity) was 1.25. However, a study performed by Sundstrand using Freon-114 in a 15.9 mm pipe resulted in C_o = 1.06. These two contradictory results proved that a more detailed understanding of slug flow is required for predicting the coefficient C_o.

Bousman, McQuillen, and Witte (1996) present a paper describing the effects of tube diameter, liquid viscosity, and surface tension on microgravity two-phase flows in regards to flow regime transitions. The tests were carried out on two different zero-g aircraft with subtly different flow loops. The first loop was flown on the Model 25 Learjet out of NASA Lewis Research Center. The development length for the system was 86 pipe diameters (963.2 mm) and had a 12.7 mm ID test section for observation

and recording. After exiting the test section the flow enters a gas-liquid separator where the liquid is recycled and the air is vented into the cabin of the reduced gravity aircraft. The second test loop was constructed for the KC-135 zero-gravity aircraft based out of NASA Johnson Space Center. This test loop utilized the same metered flow rates of air and liquid to the mixer used in the Learjet loop and used pipe with an ID of 25.4 mm. The KC-135 loop also incorporated a recycle system for the liquid to refill the liquid storage tank since the KC-135 was capable of performing many more trajectories per flight than the learjet (Bousman 1994). Measurements recorded in their analysis include void fraction, liquid film thickness, and pressure drop for three liquid gas combinations: air/water, air/water-Glycerin, and air/water-Zonyl. High speed video imagery was recorded. Their results suggest that the transition between the bubbly and slug flow regime is controlled by surface tension, and liquid velocity for air-water systems as their transition is based upon a critical void fraction and bubble packing theory. They also suggest that the transition between the slug and annular flow regimes is not dictated by tube diameter, surface tension, and liquid viscosity in the regions of their test data. Data were collected over a range of flow regimes; however, values for the void fraction were only presented for the bubbly and slug regimes. The authors presented a value of 1.2 for the distribution parameter and neglected a value for the drift velocity which is assumed to be zero.

In 1997, the ITP group conducted two-phase experimentation using R-134a, also called Suva, as the working fluid and gas to test void fraction sensors and collect void fraction data under microgravity conditions. This was followed by the development of a

statistical method for analyzing void fraction fluctuations as a possible way to identify flow regimes (Chang 1997). The testing was done aboard the KC-135 Zero-G aircraft from Johnson Space Center. The flow loop used in the experiment had sub-cooled Suva enter a bored rod evaporator that would produce the two-phased mixture. The two-phase flow then passed through the test section consisting of an upstream void fraction meter, a quick closing valve, a flow visualization tube, a second quick closing valve, and a downstream void fraction meter. Upon exiting the test section the Suva entered a condenser to be cooled down to sub-cooled liquid. The quick acting valves isolated the two-phase flow in the tube while bypassing the test section and enabling the loop to maintain constant system conditions. After isolation, the test section was rotated from its normal horizontal position to a vertical position to measure the liquid level in the sight tube. The test section has an inner diameter of 10.4 mm and a test length of 140 cm. There was not a developing length as the flow went through a one hundred and eighty degree bend in the pipe before entering the test section. A flow meter and pressure gauge mounted after the Suva pump measure the flow rate and pressure of the system respectively. Data for a wide range of flow regimes was collected but it should be noted that determining the flow rates was difficult due to non equilibrium performance of the boiler during the various acceleration periods of the aircraft. The transitions from microgravity parabolas to 2 g pullouts resulted in superheated flashing of the Suva. This caused the gas flow data to be suspect.

Elkow and Rezkallah (1997) produced a paper on using a capacitance sensor to measure the void fraction for normal gravity and microgravity conditions. The

microgravity portion of the testing was done on NASA's KC-135 aircraft. The flight package had a vertical test section and measured pressure, void fraction and temperature as well as a vertical viewing section. The inner diameter of the pipe was 9.53 mm and had a test length of 1050 mm (95.3 D). In this loop two-phase flow exited the mixer and travelled up the test section passing two pressure gauges at 28.1 cm and 58.6 cm and then reached the void fraction sensor 62 cm downstream from the mixer. The void fraction sensors used were a helically wound electrode sensor and a concave plate electrode sensor. The concave plate sensor was created in order to solve multiple problems with the helically wound sensor. Some of these problems were poor sensitivity, poor shielding, and a nonlinear response. Elkow and Rezkallah provided a value of 1.25 for the distribution parameter and no value for the drift velocity. It had been stated previously that buoyancy effects in microgravity would be minimal and thus the drift velocity term in the drift flux model can be ignored. With this assumption the distribution coefficient can be calculated by plotting the void fraction versus the superficial gas velocity divided by the total superficial velocity and setting the y intercept of the trendline to 0.

Lowe and Rezkallah (1999) carried out studies to measure volumetric void fraction in a 9.525mm diameter test section with a capacitance probe aboard the NASA Lewis DC-9 microgravity aircraft. The center of the void fraction sensor for this experiment was placed 685 mm (72 D) from the mixing section. Following the sensor was a viewing section with a NAC high speed video camera (1000 fps). Next were two film thickness probes separated by 3 D, the first of which is located 105 cm (110 D)

from the mixer. The air water system also recorded absolute pressures, temperature, film thickness, visualized flow regimes, and liquid and gas flow rates within the test sections. The void fraction and film thickness data were recorded at 1024 Hz. Flow rates were recorded at 70 Hz.

Zhao and Hu (2000) submitted a paper focusing on the microgravity transition of flow from slug to annular. This paper analyzed microgravity data from other sources to construct a model for the slug to annular transition in microgravity two-phase flow. Multiple previous works examined the drift-flux model in microgravity for slug flow resulting in a distribution parameter, C_o = 1.2 but Zhao and Hu found C_o = 1.16 based on the experimental result for bubble flows in microgravity testing (Colin 1996) and numerical simulations in zero gravity conditions. They also found C_o to be independent of mixture velocity. The determination of the distribution parameter was supported with the analysis of multiple working fluids, tube diameters, and experimental data. The importance of this paper to the subject is the effect of the slug to annular transition phase when analyzing slug flow data. If data is in the slug-annular region it will interfere with the statistical tests, creating outliers and reducing the accuracy of the tests.

Crowley and Chen (2001) explained results from two-phase R-12 microgravity experiments in their paper. The test bed was developed and flown by the Interphase Transport Phenomena lab group from Texas A&M University. This test bed utilized a two-phase pump and Coriolis flow meters to produce well characterized two-phase flow in a 12.7 mm diameter test section. Void fraction was measured using two capacitance sensors at the inlet and exit of the test section that had three void fraction measurement

points: a 3 mm ring, a 6.5 mm ring and a 135 mm volume-average sensor. High speed imagery was also recorded. The authors specifically used the drift-flux model to analyze data collected in the slug flow regime. In their analysis, they determined a value for the distribution parameter and neglect the effects of the drift-velocity. They showed similar results to an air-water experiment conducted by Bousman in comparison with their slug flow regime data. The end result of this paper was the production of the Creare flow regime map which defined the flow transition from slug to annular based on a constant gas velocity. A point to note about this regime map is that it does not develop the bubbly to slug flow transition because the transit time of fluids in the test facility was longer than the microgravity period. Therefore the Creare flow regime map uses the previous bubbly-slug transition proposed by Lee where there is a critical void fraction between 0.2 and 0.45 at which the transition occurs.

Clarke and Rezkallah (2001) presented a study of the drift-velocity for the bubbly flow regime at microgravity for air and water. The authors showed results from numerical simulations of the bubbly flow regime produced in their microgravity experiment. The simulation predicted similar results for the drift-velocity of their flows and also for the rate at which bubbles move towards the centerline of their test section. They determined that significant factors in determining the value of the drift-velocity include bubble diameter, radial bubble position, the liquid Reynolds number, and finally the tube diameter. They found that higher drift-velocities are the result of the elongation of larger shaped bubbles in the tube. In addition, bubbles in larger tubes do not experience the same liquid shear as in smaller tubes, and therefore these flows have

smaller drift-velocities. Another factor in decreasing the drift-velocity is an increase in the surface tension which also causes less bubble elongation. Finally, the authors stated that surface tension forces act against the liquid viscous forces in order to maintain spherically-shaped bubbles meaning that higher surface tension forces in the two-phase flow result in a smaller drift-velocity as well.

Choi, Fujii, Asano, and Sugimoto (2002) conducted two-phase flow experiments and compared the microgravity data and flow characteristics to 1g and 2g data. The microgravity tests were conducted aboard the MU-300 aircraft. The test section consisted of 10 mm tubing over a 600 mm testing length. A 500 mm developing length was included to allow flow to come to equilibrium before entering the test section. Directly after the test section was another 300 mm section that was equipped with a void fraction probe at the midpoint. Knowing the void fraction and flow rates, the authors constructed a plot of superficial gas velocity divided by void fraction vs. the total mixture superficial velocity. The significance of this plot is that the slope of the line is the drift flux parameter C_o. The analysis preformed on the data resulted in a $C_o = 1.29$. The author did not have Choi's numerical data to use in this thesis' analysis, instead the data was extracted from Choi's plot of the superficial velocities and Choi's plot of the void fraction weighted superficial gas velocity versus the superficial mixture velocity. One other point of interest in Choi's paper is that it notes their observed void fractions were larger than the Inoue-Aoki model.

Valota (2004), an ITP researcher, published his thesis on identifying the flow pattern based on statistics, Martinelli analysis, and Drift Flux analysis. This research

was based on the data collected from the Crowley and Chen (2001) research flight in 2001 using R12 data. The statistical tests for variance and signal to noise ratio were found to be good flow pattern indicators. From the Martinelli analysis it was concluded that the slug flow has a different trend in comparison with annular an in general the Martinelli analysis was a good flow pattern identifier. Of note is that this study only included void fraction data from the 3 mm ring sensor used in the experiment providing a very narrow band to record the volume-averaged void fraction. The Drift Flux model produced a C_o value of 1.1 and a u_{gj} value of 0.21. Braisted (2004), also an ITP researcher, published another thesis on the drift flux based on the data collected from the Crowley and Chen (2001) experiment. This work produced a C_o value of 1.54 and a u_{gj} value of -0.1.

Reinharts (1993), through his dissertation work at Texas A&M and the ITP, developed a new model for flow regime transition from slug to annular flow in microgravity. His work showed that thicker liquid films are present in microgravity which forces the Taylor bubbles in slug flow into a more parabolic shape instead of a hemispherical shape. This is important as the thicker films force the bubbles to travel faster through a narrower area in the flow channel. This was also pointed out in research by Wheeler (1992) and Nguyen (2009). It was noted in Nguyen that the liquid film has higher average velocity than in normal gravity and that the liquid movement is effected by the momentum of the gas.

In 2004 the ITP (Neill unpublished) flew a slip correlation test bed on board the KC-135 that measured void fraction of a water-nitrogen mixture by using quick acting

valves to trap the liquid and gas volume inside a 12.7mm diameter test section. The water was pumped by a micro pump gear pump and the gas was supplied by a compressed nitrogen cylinder, and the flow was mixed in a single T-junction. This loop had no developing length due to the right angle turn in the piping to enter the quick acting valves. The test section was 1168 mm long and flowed into a two-phase separator to recycle the gas and liquid in the system. To measure the void fraction of the flow, the test section was isolated using the quick acting valves near the end of the 0g parabola. The liquid levels were measured in the vertical tube during the 2-g period of the flight allowing for the calculation of void fraction. After the measurement was taken the valves were reset in preparation for the next parabola. Gas and liquid flow rates were measured independently using laminar plate flow meters.

Table 1.1 shows information about the different experimental data collected to generate this data set. The data includes nine different authors and thirteen different test setups which provide 398 individual data points for the analysis. The table also shows the reported C_o and u_{gj} values for each researcher. This data was compiled into a simple database for use in the statistical method and the drift flux model. These researchers developed their values for the drift flux model based only on their own collected experimental data, even when multiple data sets are analyzed, they are analyzed separately and no attempt to combine the data is made. This means the developed drift flux models are susceptible to any biases that may have been present in the experiment. This can be seen as the bubble distribution parameter for water and air data ranges from 1.2 to 1.48 between the researchers. This adhoc approach to developing the drift flux

model is driven by availability of data, but this research aims to eliminate that approach by looking at a large volume of data and using a statistically consistent method for determining the drift flux parameters.

1.3 THESIS ORGANIZATION

The next chapter details the development of the drift-flux model for microgravity two-phase flow. Chapter 3 explains the rigor of the statistical method used for this research and why the application of these statistics is critical to microgravity two-phase flow. Chapter 4 details the results of applying the statistical analysis to the collected data and the development of one statistically valid data set generated from the combined data of multiple researchers listed in Chapter 1. Chapter 5 describes the results of the analysis and the development of a comprehensive drift-flux model for zero-g two-phase flow. Chapter 6 consists of a summary, conclusions and recommendations drawn from this research.

Table 1.1 Summary of Reduced Gravity Experiments

Author	Year	Gravity	Micro-gravity Simulator	Liquid	Gas	C_o	u_{gj}	Diameter [mm]	Test Length [mm]	Void Fraction Technique
Zuber[a]	1965	1g	N/A	Water	Air	1.2	0-3	-	-	-
França[a]	1992	1g	N/A	Water	Air	1.2	-0.2	19	1830	Quick Acting Valves
Braisted[a]	2004	µg	KC-135	R12	R12	1.54	-0.1	12.7	1630	Capacitance Probe
Valota[a]	2004	µg	KC-135	R12	R12	1.1	0.21	12.7	1630	Capacitance Probe
Dukler	1987	µg	Lewis 100 ft. Drop tower Lewis Learjet	Water	Air	d	d	9.52 12.7	457 1060	Reynolds Number and Shear Stress Relation
Colin[e]	1991 1994	µg	Airbus A300	Water	Air	1.2 1.2 1.2 1.2	0 0 0 0	40 6 10 19	3170 480 800 1520	Conductivity Probe
Elkow	1994	µg	KC-135	Water	Air	1.25	c	9.53	908	Capacitance Sensor
Bousman	1995	µg	Model 25 Learjet	Water w/Zonyl w/Glycerin	Air	1.21 1.21 1.48/ 1.21	c	12.7	640	Conductivity Probe
Chang	1997	µg	KC-135	R134a	R134a	d	d	10.4	1400	Capacitance sensors and quick acting valves
Lowe	1999	µg	Lewis DC-9	Water	Air	1.28	0	9.525	1050	Capacitance Sensor
Crowley	2001	µg	KC-135	R12	R12	1.3	c	12.7	1630	Capacitance Probe
Choi	2002	µg	MU-300	Water	Air	1.29	-0.19	10	600	Void Fraction Probe
Neill	2004	µg	KC-135	Water	Air	d	d	12.7	1168	Quick Acting Valves

a Denotes researchers whose data is not used in this analysis but have recorded results using the drift flux model for comparison.
b assumed model of 1.2 and 0
c not reported assumed to be 0
d not calculated
e. These data points come from Colin, Fabre, and Duckler (1991) and Colin, Fabre, and McQuillen (1996).

CHAPTER II

DRIFT-FLUX DEVELOPMENT

2.1 INTRODUCTION

This chapter describes the development of the drift-flux model for two-phase flow and how the model, along with distribution parameter and drift flux, are used to calculate void fraction. All two-phase flows involve some relative motion between the phases, thus the flow can be defined by a set of equations with respect to the velocities of each phase.

2.2 DERIVATION OF THE DRIFT FLUX MODEL

The gas and liquid volumetric flux densities are defined by Equations 3 and 4.

$$j_v = \alpha u_v \tag{3}$$

$$j_l = (1-\alpha)u_l \tag{4}$$

Where α represents the void fraction, u_v represents the gas velocity and u_l represents the fluid velocity. The equations below have $\langle\,\rangle's$ which denotes the average over a cross section. The area-average of a quantity, F, over the cross-sectional area, A, is defined by Equation 5.

$$\langle F \rangle = \frac{1}{A}\int_A F dA \tag{5}$$

The area-averaged volumetric flux densities for the liquid and gas are defined by taking the averages of Equations 3 and 4.

$$\langle j_v \rangle = \langle \alpha u_v \rangle = \frac{Q_v}{A} \tag{6}$$

$$\langle j_l \rangle = \langle (1-\alpha) u_l \rangle = \frac{Q_l}{A} \tag{7}$$

Where Q_{gv} is the gas volumetric flow rate, Q_l is the liquid volumetric flow rate, and A is the cross-sectional area of the test section. These average volumetric flux densities are referred to as superficial velocities.

The relative velocity, v_r, is the difference in velocity of the phases at a given radial position in the channel shown in Equation 8.

$$u_r = u_v - u_l \tag{8}$$

The drift velocity of the gas, j_{gj}, is defined as the velocity of the gas with respect to the volumetric flux density of the mixture, j, as stated in chapter 1 and the definition is shown below from Collier (2002).

$$j_{gj} = \alpha(1-\alpha)u_r = \alpha(1-\alpha)j_v - \alpha j_f = j_v - \alpha j \tag{9}$$

The void-fraction-weighted mean drift-velocity is given by:

$$u_{gj} = \frac{\langle j_{gj}\rangle}{\langle\alpha\rangle} = \frac{\langle\alpha j_v\rangle}{\langle\alpha\rangle} - \frac{\langle\alpha j\rangle}{\langle\alpha\rangle} \tag{10}$$

The standard formulation for the one dimensional drift-flux model can be derived by rearranging Equation 10 to give Equation 11.

$$\frac{\langle j_v\rangle}{\langle\alpha\rangle} = \frac{\langle\alpha j\rangle}{\langle\alpha\rangle\langle j\rangle}\langle j\rangle + \frac{\langle\alpha v_{gj}\rangle}{\langle\alpha\rangle} = C_o\langle j\rangle + u_{gj} \tag{11}$$

Where C_o and u_{gj} are the distribution parameter and the void-fraction weighted mean drift velocity. The distribution parameter is defined in Equation 12 as:

$$C_o = \frac{\langle\alpha j\rangle}{\langle\alpha\rangle\langle j\rangle} \tag{12}$$

From chapter 1, the bubble distribution parameter accounts for the uneven distribution of phases across the flow channel. This portion is on the development of the bubble distribution parameter C_o. Zuber and Findlay (1965) developed a general

expression for predicting the average volumetric concentration that takes into account the effect of non-uniform flow and concentration profiles as well as the effect of the local relative velocity between phases. Zuber defines this distribution parameter as shown in Equation 13.

$$C_o = \frac{\langle \alpha j \rangle}{\langle \alpha \rangle \langle j \rangle} = \frac{\frac{1}{A}\int_A j\alpha dA}{\left[\frac{1}{A}\int_A j dA\right]\left[\frac{1}{A}\int_A \alpha dA\right]} \tag{13}$$

Zuber references the previous work of Nicklin, Wilkes, and Davidson (1962) as one of the attempts to account for the effect of non-uniform flow distribution on the volumetric concentration. Nicklin et al. (1962) state that C_o = 1.2 is derived from the ratio of the maximum to the average flow velocity being 1.2. This derivation does not account for phase concentration profile but does give insight to the 1.2 value.

Zuber and Findley investigated the effects of non-uniform flow and concentration distribution on the value of the phase distribution parameter analytically. For simplicity, they consider an axially symmetric flow through a circular duct and assume that the flow and concentration distributions are given by:

$$\frac{j}{j_c} = 1 - \left(\frac{r}{R}\right)^m \tag{14}$$

And

$$\frac{\propto - \propto_w}{\propto_c - \propto_w} = 1 - \left(\frac{r}{R}\right)^n \tag{15}$$

The term *á* represents void fraction and the subscripts *c* refers to the value evaluated at the center line and *w* refer to the value evaluated at the wall of the tube. The exponent *m* represents the exponent for velocity distribution while *n* represents the exponent for void distribution in the above equations.

The first step to calculating the bubble distribution parameter from Equation 11 is to calculate the centreline volumetric flux, j_c, from Equation 14 using Equation 16 below.

$$j_c = \frac{Q_v}{\pi r^2} \tag{16}$$

The mass flow rate of the gas is represented by Q_g. The radius of the gas core, r, is calculated using the relationship between Equation 14 and 15:

$$\alpha = 1 - \left(\frac{r}{R}\right)^m = \frac{j}{j_c} \tag{17}$$

Where R is the radius of the pipe, j is the mixture velocity, and m is the exponent on velocity distribution. Using the equality from Equation 17 and the value for j_c from Equation 14 the void fraction is equal to Equation 18.

$$\alpha = \frac{j}{\frac{Q_v}{\pi r^2}} \tag{18}$$

Solving Equation 18 for the gas core radius gives Equation 19. All variables on the right hand side of the equation are known.

$$r = \sqrt{\frac{\alpha Q_v}{\pi j}} \tag{19}$$

With j_c and r calculated, the velocity distribution, m, can be solved by rearranging Equation 17 for m where r^* is the ratio of the gas core radius to the pipe radius.

$$1 - r^{*m} = \frac{j}{j_c} \tag{20}$$

$$-r^{*m} = \frac{j}{j_c} - 1 \tag{21}$$

$$r^{*m} = 1 - \frac{j}{j_c} \tag{22}$$

$$m \ln(r^*) = \ln\left(1 - \frac{j}{j_c}\right) \tag{23}$$

$$m = \frac{\ln\left(1-\frac{j}{j_c}\right)}{\ln(r^*)} \tag{24}$$

Next is solving for the void distribution using Equation 15. Using the assumptions that void fraction at the centreline is always 1 and void fraction at the wall is always 0 Equation 15 is reduced to Equation 25. Then the equation is solved for *n* as shown in Equation 29.

$$1 - r^{*n} = \alpha \tag{25}$$

$$-r^{*n} = \alpha - 1 \tag{26}$$

$$r^{*n} = 1 - \alpha \tag{27}$$

$$n \ln(r^*) = \ln(1 - \alpha) \tag{28}$$

$$n = \frac{\ln(1-\alpha)}{\ln(r^*)} \tag{29}$$

Using these values for m and n the following equation calculates C_o. The following equation is for the distribution parameter C_o when expressed in terms of the volumetric concentration $\acute{a}_w$ at the wall.

$$C_o = 1 + \frac{2}{m+n+2}\left[1 - \frac{\alpha_w}{\langle\alpha\rangle}\right] \tag{30}$$

The following is the expression of the distribution parameter in terms of the volumetric concentration $\acute{a}_c$ at the center line.

$$C_o = \frac{m+2}{m+n+2}\left[1 + \frac{\alpha_c}{\langle\alpha\rangle}\frac{n}{m+2}\right] \tag{31}$$

Figure 2.1 shows various laminar and turbulent profiles with the value of C_o computed from Equation 30 and 31 plotted against the ratio of the volumetric concentration of the wall over the volumetric concentration of the center line. The C_o = 1.2 that has been historically observed is the result of one of the exponents exhibiting a flat profile across the bubble (Zuber and Finley 1965). This figure captures the effect of the velocity and void fraction profiles on the distribution parameter. For the more pronounced parabolic profiles, the distribution parameter reaches a value of C_o = 1.5; whereas it trends towards a value of unity for flat profiles. The hemispherical shape of the bubbles is discussed in depth in the research of Davies and Taylor (1950). This has been well documented; however in microgravity the bubble shape is much more parabolic as shown in Reinarts (1993).

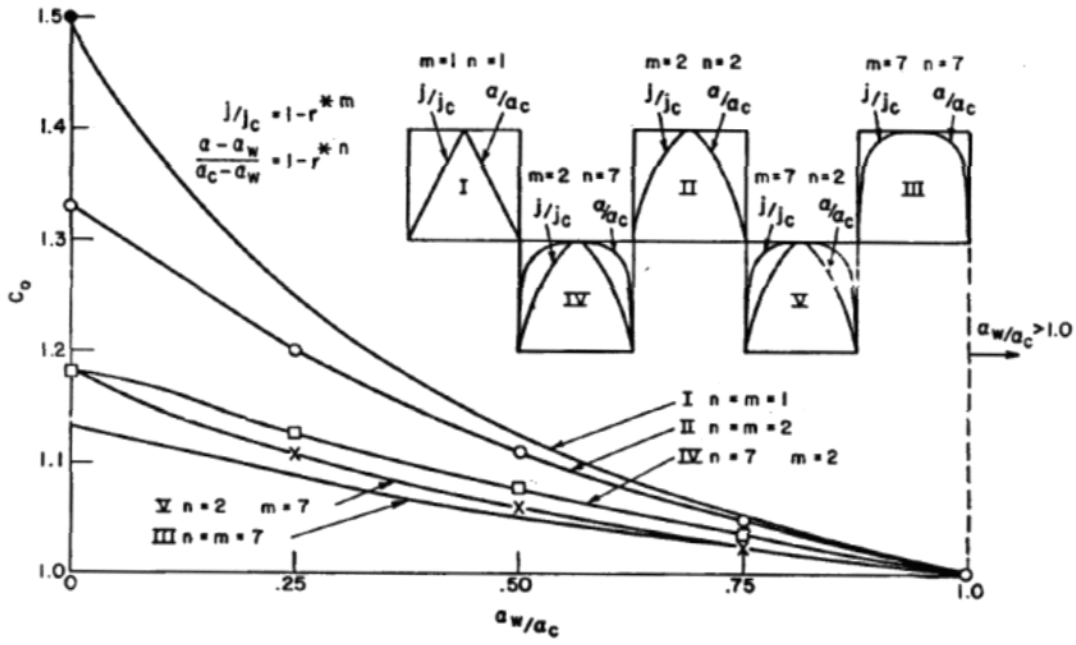

Figure 2.1 Distribution Parameter Values as a Function of the Exponents of the Flow and Concentration Profile

The drift velocity from Equation 9 represents the volumetric flux of the gas relative to the volumetric flux of the mixture. The equation for determining the Drift Velocity, V_{gj}, comes directly from the derivation of the drift flux model and starts in Wallis (1989). This section covers rise velocity of single bubbles in stagnant liquid and details terrestrial two-phase vertical up flow. The rise velocity is determined by the interaction between buoyancy and the other forces acting on the bubble due to shape and motion. If the bubble viscosity is negligible, the only other forces that are important are liquid inertia, liquid viscosity, and surface tension. The balance between buoyancy and these three forces are expressed in terms of three dimensionless groups:

$$\pi_a = \frac{\rho_f v_\infty^2}{Dg(\rho_f - \rho_{gv})} \tag{32a}$$

$$\pi_b = \frac{v_\infty \mu_f}{D^2 g(\rho_f - \rho_{gv})} \tag{32b}$$

$$\pi_c = \frac{\sigma}{D^2 g(\rho_f - \rho_v)} \tag{32c}$$

Where v_∞ is the terminal velocity in an infinite medium, D is a characteristic dimension of the duct cross section, g is gravity, ρ_f and ρ_g are the density of the fluid and the gas, μ_f is the fluid viscosity, and σ is the surface tension. The general solution is a function of these three parameters. The simplest solution is when only one dimensionless group governs the motion. The inertia dominant case is given solely in terms of the first dimensionless group which is shown in Equation 33. The second (32b) and third (32c) terms which correspond to the viscous and capillary forces respectively are assumed to be negligible.

$$v_{\infty} = k_1 \left[\frac{gD(\rho_f - \rho_g)}{\rho_f}\right]^{1/2} \quad (33)$$

Equation 33 shows a generic rise velocity equation based on inertia and buoyancy. The constant k_1 = 0.351 in the equation was obtained through experimental results for two-phase vertical up flow in a terrestrial environment by Dumetrscu (1943). This experimental constant defines Equation 33 as the empirical model in Equation 34 and has been the major assumption for calculating a gravity dependent drift velocity. This equation is the terminal velocity for a bubble rising in a stagnant liquid for vertical upflow. This equation is used to define the drift velocity in vertical upflow in the drift flux model by empirically fitting a constant to the terminal rise velocity equation. Since buoyancy force approaches 0 in microgravity the general conclusion for the drift flux model is that u_{gj} also approaches 0. Several researchers have reported this as the drift velocity whether it has been calculated or assumed. However, this empirical model was never validated against microgravity data and the absence of gravity means that the other forces which were once negligible have to be addressed and accounted for, this will be discussed further in chapter 4.

$$u_{gj} = 0.351 \left[\frac{g\Delta\rho D}{\rho_f}\right]^{1/2} \quad (34)$$

This balance between the local interfacial drag and the buoyancy force is not appropriate for horizontal flow in 1-g application because of stratified flow. In horizontal flow the drift velocity is related to the phase distribution and to the local slip resulting from lateral and axial pressure gradients and that the structure of the interface determines the drift-flux parameters (Franca & Lahey 1992). A key point from this

paper is that for horizontal flows the drift velocity is not normally zero. The fact that many previous authors have assumed it to be zero just highlights their misunderstanding of what the drift velocity represents. This paper explained the negative value for u_{gj} by the displacement experienced by the gas bubble, its pressure drop expansion and the liquid velocity distribution in the slug. The liquid velocity profile is strongly distorted due to drainage around the bubble, and the liquid under the bubble flowing at a lower velocity than in the slug ahead of the bubble. Although gravity is in this term, no microgravity data is used in its development which gives rise to the assumption that drift velocity is zero under the microgravity condition.

The effects of this distortion on the velocity profile were measured in the 1984 paper by Kvernvold et Al. (1984). The experiment was designed to measure the velocity profiles and variations in both the film and the liquid slug. The major findings from that experiment that impact this analysis are that as the gas flow rate increases, the length of the film increases and the slug lengths are relatively constant. The finding relevant to this discussion is that the translational speeds of the liquid slugs are proportional to the mixture velocity as shown in Equation 35. This shows how the liquid slugs are pushed by the Taylor bubbles in slug flow and gives a proportionality constant to adjust the calculated drift velocity.

$$V_t \approx 1.52\, V_m \tag{35}$$

The void fraction weighted superficial gas velocity and the superficial mixture velocity are not difficult to obtain thorough experimentation if the experiment can measure the flow rates of each phase, the void fraction, and one knows the cross

sectional area of the test pipe. This information is used to generate a linear relationship between the void fraction weighted superficial gas velocity and the superficial mixture velocity. Under microgravity conditions the flow rate and void fraction data is collected and via assumptions made by researchers applied to develop terrestrial empirical models; however there are some concerns for this approach. These researchers tend to use only data collected from individual microgravity experiments that they themselves conducted resulting in a limited number of points in the data. Then the method for selecting and analyzing the individual points from this data does not follow a statistically consistent approach and can vary widely from researcher to researcher. Visual conformation of flow regimes is an example of this, what one may consider slug flow can be considered by another to be in the transitional state between flow regimes, or another flow regime altogether. Finally there is a tendency for researchers to force the data to conform to established terrestrial models through assumptions such as the drift velocity being zero in microgravity. The thesis work presented here shows a more statistically consistent approach to analyzing data which is used to determine the drift flux parameters. This statistical method is described in detail in the next chapter.

CHAPTER III

APPLICATION OF A LINEAR REGRESSION MODEL

3.1 INTRODUCTION

The development of the drift flux model leads to using a linear regression to obtain values for C_o and u_{gj}. This chapter describes the statistical analysis performed with the data, interpretation of the statistical results, and how analyzing these results can reduce the data set to produce a statistically consistent drift flux model. Typically, values for *Co* and u_{gj} are fitted to a linear line without consideration to the axioms of a linear model. Because the linear model will be used as a predictive model over a wide range of fluid flow values, it is important to make sure the model is statistically consistent. The focus of the statistical analysis is to validate the four axioms in a linear regression model. These axioms are that the residuals of each group are independent of each other, the mean of the residuals is zero for the data set, the residuals variance is constant, and the residuals follow a normal distribution.

A microgravity data set was compiled from multiple researchers listed in Table 1.1. This data set was analyzed using a number of statistical tests associated with demonstrating the requirements of each of the four axioms are met. When possible, non-parametric tests were used because they are more powerful tests that rely on fewer assumptions. The tests were performed on the data using the Statistical Package and Service Solutions (SPSS) software package. Figure 3.1 shows the flow chart for the work flow analysis and the associated decisions regarding the data.

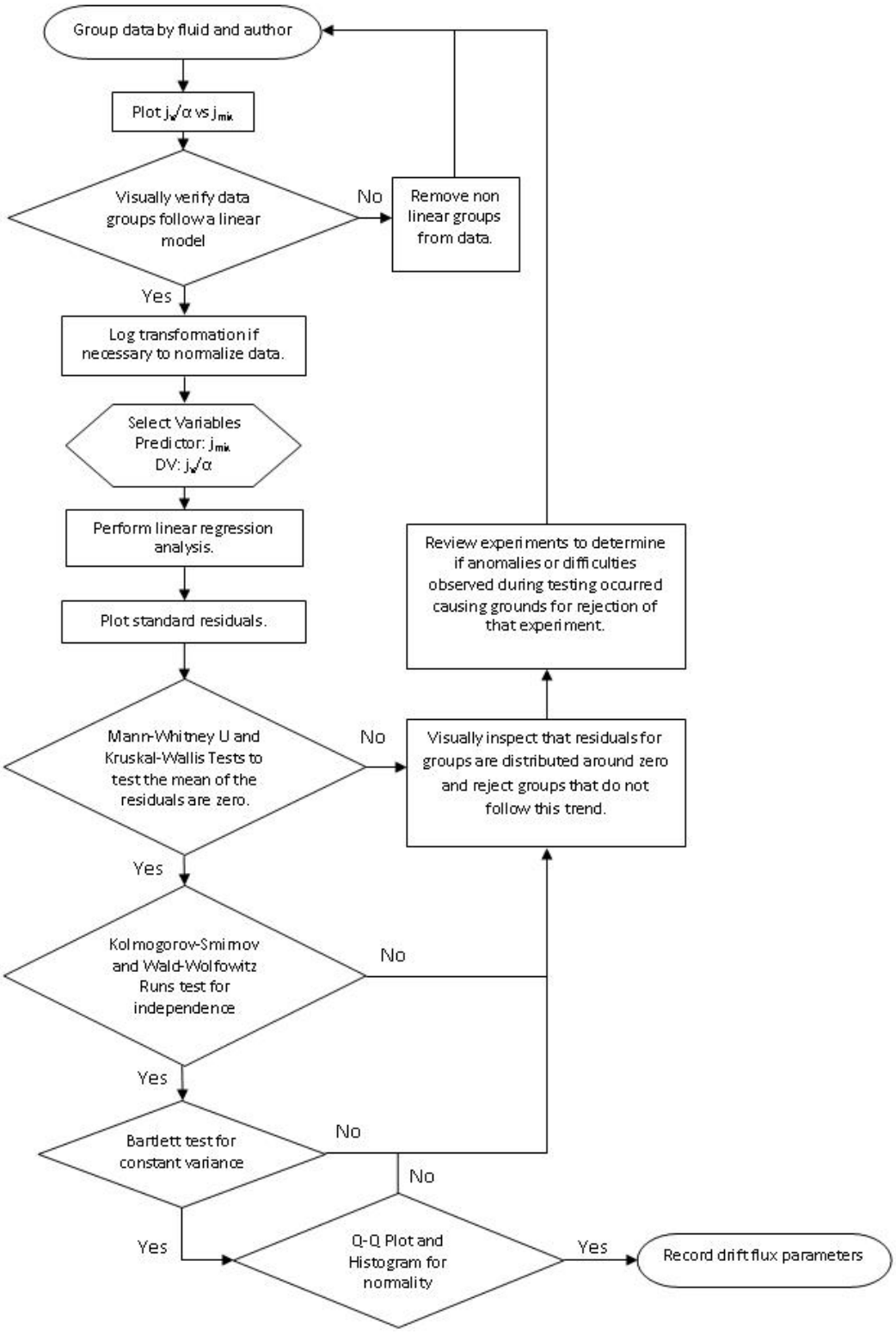

Figure 3.1 Flow Chart for Statistical Analysis

3.2 LINEAR REGRESSION ANALYSIS

A statistically consistent linear model is constructed by performing a linear regression analysis and subjecting the results to a series of parametric and non-parametric statistical tests to see if the axioms of a linear model are met. This regression generates residuals which are the vertical deviations from the estimated line. These residuals are the basis for the non-parametric tests that will be performed to determine the independence of the data sets. An evaluation of the magnitude of the standardized residuals and the Cook's distance can show if outliers are present and allow one to refine the regression. The Cook's distance shows the influence a data point has when performing a regression and measures the effect of deleting a given data point. The larger the Cook's distance the more influence the point has, and if the distance gets too large it can interfere with the regression analysis and should be examined. Since a linear relationship is being used the axioms of a linear regression needed to be evaluated for this data set. These axioms are:

1. The residuals are independent
2. The mean of the residuals is zero
3. The residuals variance is constant
4. The residuals follow a normal distribution

This is frequently referred to as an analysis of the residuals, not to be confused with residual analysis found in numerical methods. The analysis of variance (ANOVA) refers to multiple experimental situations and statistical procedures for the analysis of the different data collected from these experiments. It allows for the comparison of

results from independent experiments based on population means for a specified dependant and independent parameter. Because of the range of the data and the heavy weighting of data points in the low flow range, a log transformation was applied to the data. Data transformation refers to the application of a deterministic mathematical function to each point in a data set. The log transformation equilibrates the data along the dependent variable. The transformation distributes the data along the mixture velocity range instead of clumping at the far left in the low flow range. This means that the linear regression will be weighted evenly instead of having a low mixture velocity bias. The data can be transformed back into its original value using the inverse of the log applied to the data.

3.3 MANN-WHITNEY U TEST

The Mann-Whitney U test is a non-parametric test that is used to determine if two samples come from the same distribution and tests the axiom of if the mean of the residuals is zero. This test was used to analyze the different fluid types of the data set. Data points from both groups are combined and ranked; an average rank is assigned for ties. For cases where the populations are identical in location, the ranks should be randomly mixed between the two samples. The number of times a score from group 1 is before a score from group 2 and the number of times group 2 is before group 1 are calculated and the Mann-Whitney U statistic is the smaller of these two numbers. There were two main assumptions for this test. The first was that the samples were independent of each other and the second was observations in each sample were independent. The calculation for U is given by:

$$U_1 = R_1 - n_1 \frac{(n_1 - 1)}{2} \tag{36}$$

Where n_1 represents the sample size of sample 1, and R_1 is the sum of the ranks in sample 1.

3.4 KRUSKAL-WALLIS TEST

The Kruskal-Wallis one-way analysis of variance is a non-parametric method that tests the equality of population medians between the different groups. This test was used to verify the axiom that the mean of the residuals was zero in the linear regression. This test is also an extension of the Mann-Whitney U test to 3 or more groups and is used to analyze the data by fluid and author groups. Since the test is non-parametric it does not assume a normal population, however the test assumes that each group has identically shaped and scaled distributions. To perform this test, all data from the groups are ranked from 1 to N ignoring group membership, giving tied values the average of the ranks they would get if not tied. The test statistic is tabulated by:

$$p = (N - 1) \frac{\sum_{i=1}^{g} n_i (\bar{r}_i - \bar{r})^2}{\sum_{i=1}^{g} \sum_{j=1}^{n_i} (r_{ij} - \bar{r})^2} \tag{37}$$

Where n_i is the number of observations in group i, r_{ij} is the rank of observation j from group i, and N is the total number of observations across all groups. The target value for p is 0.05 or smaller meaning that there is no evidence for differences between the samples. For this analysis it shows that the residuals are centred on a mean value which is shown in chapter 4.

3.5 KOLMOGOROV-SMIRNOV Z TEST

The Kolmogorov-Smirnov (KS) Z test is a non-parametric test used to determine if two probability distributions differ or if a probability distribution differs from a hypothesized distribution. The two-sample KS test is sensitive to differences in both the location and shape of the distribution function of the two samples and can be used to determine if the residuals are independent. For this thesis, the KS test is a type of minimum distance estimation that compares two samples and was chosen based on the number of data points in the population and is passed if the *p* value reported is above 0.05.

3.6 WALD-WOLFOWITZ RUNS TEST

The Wald-Wolfowitz test is a non-parametric test used to check that the elements of the sequence are mutually independent. A run of a particular sequence is a segment of the sequence made of adjoining equal elements. An example of this is the sequence is shown below in Figure 3.2 and consists of five runs, three run of +'s and two runs of –'s

+ + – – – – – + + + + – – – – – – + + + + +

Figure 3.2 Example Sequence for Runs Test

3.7 Q-Q AND HISTOGRAM PLOTS

A good qualitative method to test for normality is to generate a normal Q-Q plot of the standardized residuals. The use of Q-Q plots to compare samples can be viewed as a non-parametric approach to comparing the underlying distributions. This plot is

generated with the standard residual on the ordinate and the theoretical quantiles on the abscissa. If the resulting plot is close to a straight line then the data is said to be consistent with that from a normal distribution. The histogram can also be used to test if the residuals follow a normal distribution. If there are multiple peaks in the histogram plot then there is a departure from normality. The desired plot is a single peak centered on zero to represent a normal distribution.

3.8 BARTLETT TEST

Bartlett's test is used to test if n samples have equal variance. Because Bartlett's test is sensitive to departures from normality, it can also be used to test for non-normality. This test is used to validate the third assumption of the linear regression, that the residuals variance is constant. Bartlett's test is used to test the null hypothesis that all k populations' variances are equal if the *p* value is below 0.05.

3.9 SUMMARY

Using the work flow shown in Figure 3.1 and the above mention tests, one shows how to test the accumulated data for the axioms for a linear model. By proving that the residuals of each group are independent of each other, the mean of the residuals is zero for the data, the residuals variance is constant, and the residuals follow a normal distribution one creates a consistent evaluation for analyzing data from multiple sources. Using these tests resulted in a reduced data set that meets the axioms and produced a linear model that fits the data.

CHAPTER IV

STATISTICAL RESULTS

4.1 INTRODUCTION

This chapter applies the work flow generated in chapter 3 to the research data from Table 1.1 in chapter 1. The tests described in the work flow are used to reduce the collected data down to a statistically valid data set that adheres to the axioms of a linear model.

4.2 DATA ANALYSIS

The slug flow data from the researchers in Table 1.1 was compiled into a single data set to undergo an extensive statistical analysis as described by the flow chart in Figure 3.1 from Chapter 3. The data from Table 1.1 is presented in Figure 4.1, which is a plot of the average superficial gas velocity divided by the void fraction versus the mixture velocity. The N^2 in the legend of the plot represent the nitrogen gas used to simulate air in the system during testing. The data for R134a shows a strong nonlinearity with increasing mixture velocity. This is due to the inaccuracy of determining the individual phase flow rates through the boiler system (Chang 1997). Another concern is that higher mass fluxes require higher electrical power to produce the desired quality increases leading to sharper transients from the parabolic flight profile which leads to superheating due to flow regime changes from 0 g to 2 g transitions. Therefore the R134a data can be removed due to the large uncertainty in the phase velocities. The remaining data points undergo the log transformation and statistical tests.

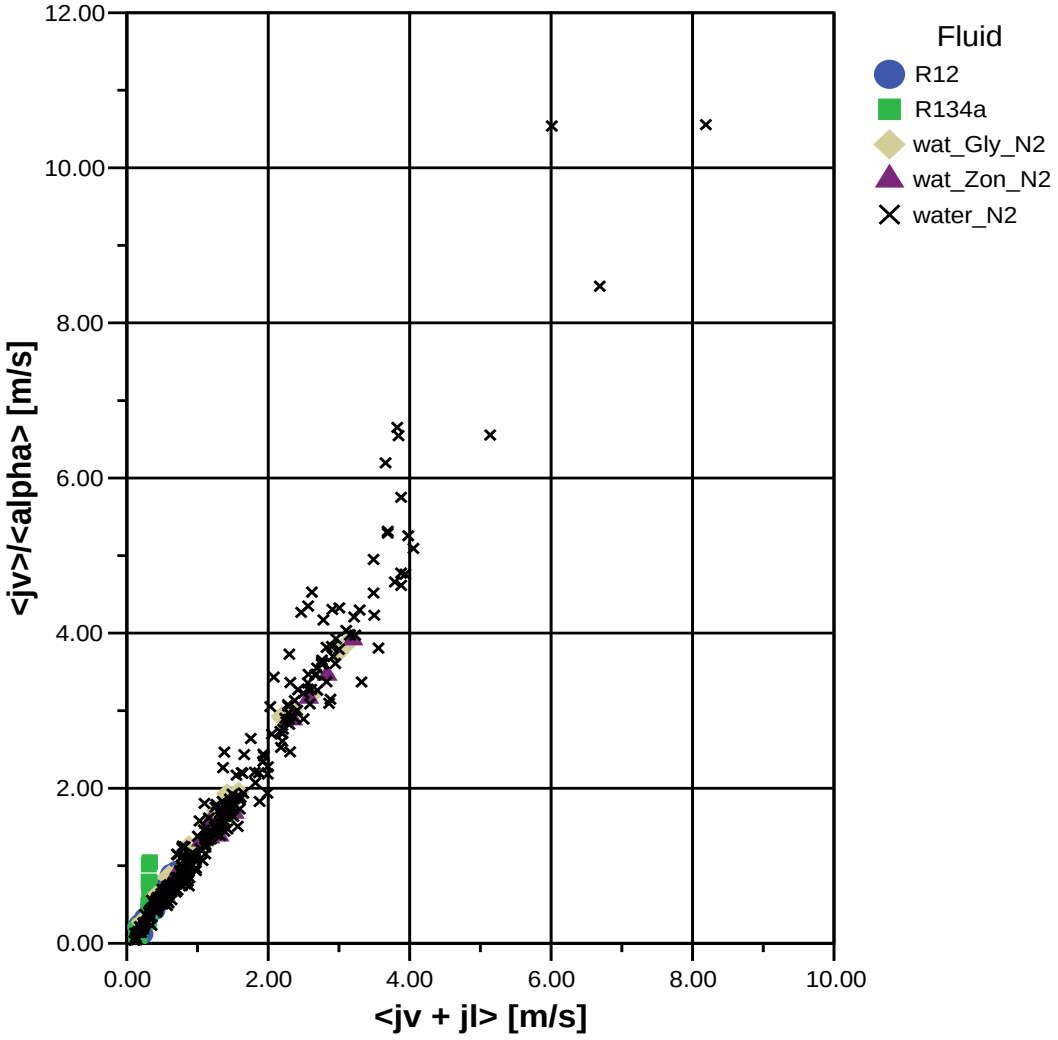

Figure 4.1 Slug Flow for Various Fluids

The next step is to transform the data into a log base 10 data set. The transformation enables the data to be equilibrated along the line, where as Figure 4.1 contains the majority of the data points massed together in a small area. This is done by taking the log base 10 of the superficial mixture velocity and the log base 10 of the superficial gas velocity divided by the void fraction. The transformed data set is shown

in Figure 4.2. The data then undergoes a linear regression and the residuals are plotted in Figure 4.3.

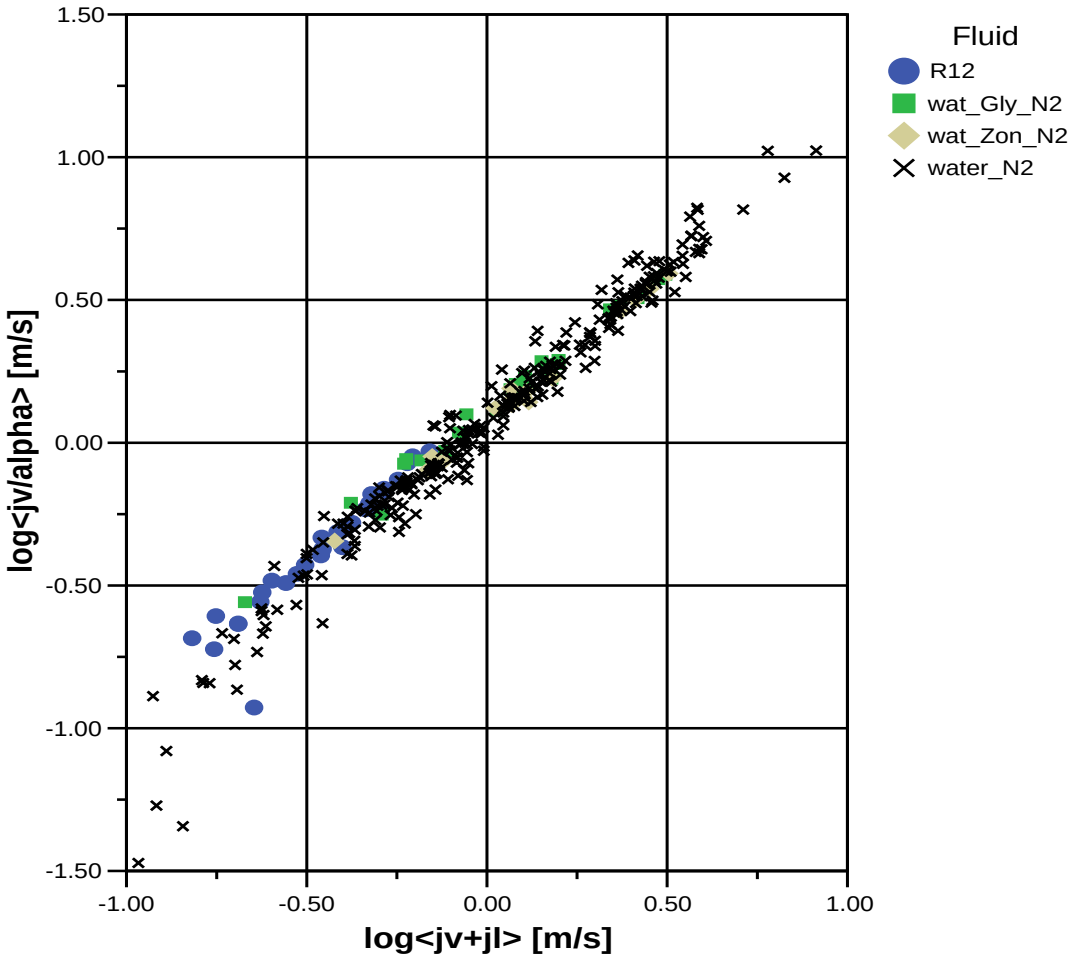

Figure 4.2 Log Transformation of Slug Flow Data

Looking at Figure 4.3 it can be seen that the R12 data and the water-Glycerin/air data residuals are not distributed around zero. This is further supported by the non-parametric tests which indicate that both fluids have different means and distribution

shapes. The fluid groups do not pass the Kruskal-Wallis test with all four groups. However the water/air and water-Zonyl/air fluid groups pass both the Kruskal-Wallis test and the Kolmogorov-Smirnov tests. Thus R12 and the water-Glycerin/air groups are removed from the data set leaving only the water/air and water-Zonyl/air data.

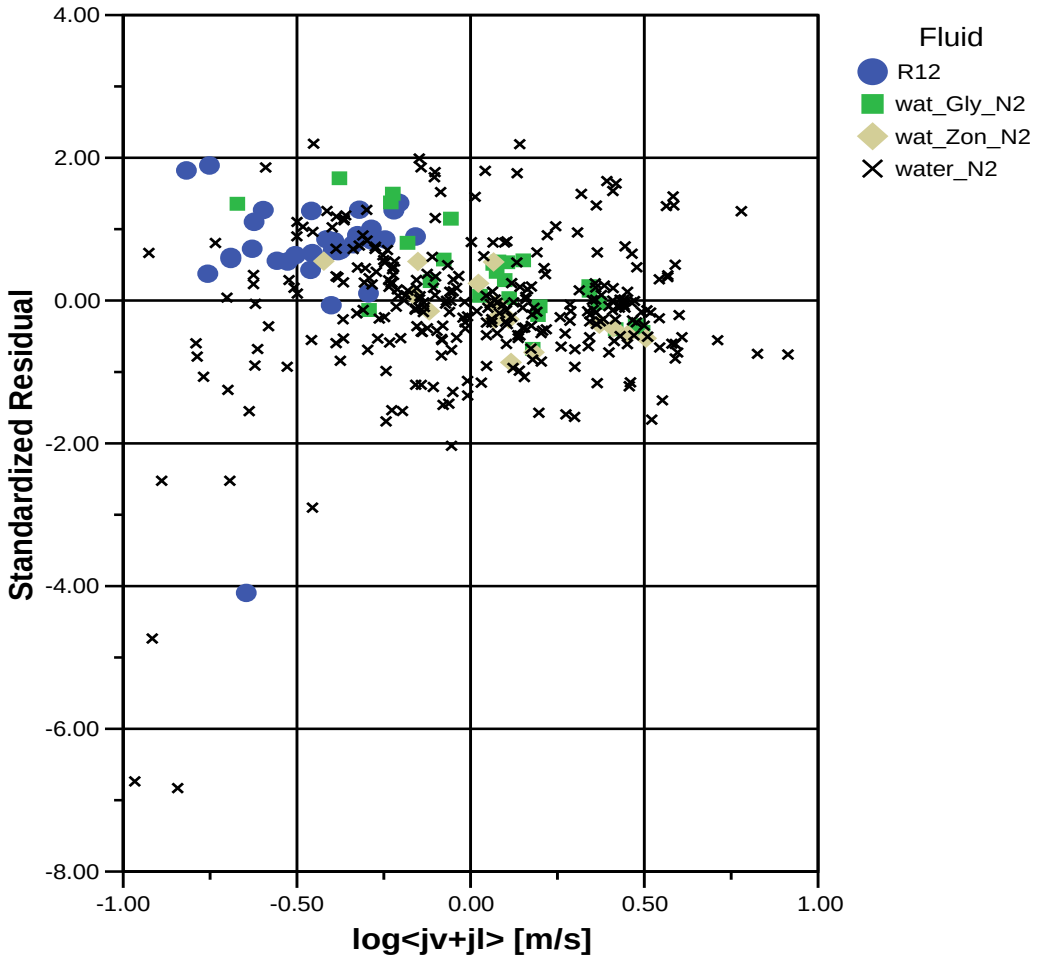

Figure 4.3 Standard Residuals vs. Log Mixture Velocity

The remaining data set was sent back to the beginning of the flow chart from Figure 3.1 and the data was separated into groups based on the individual experiments.

This grouping can be seen in Figure 4.5 where the points are labelled by the author's name.

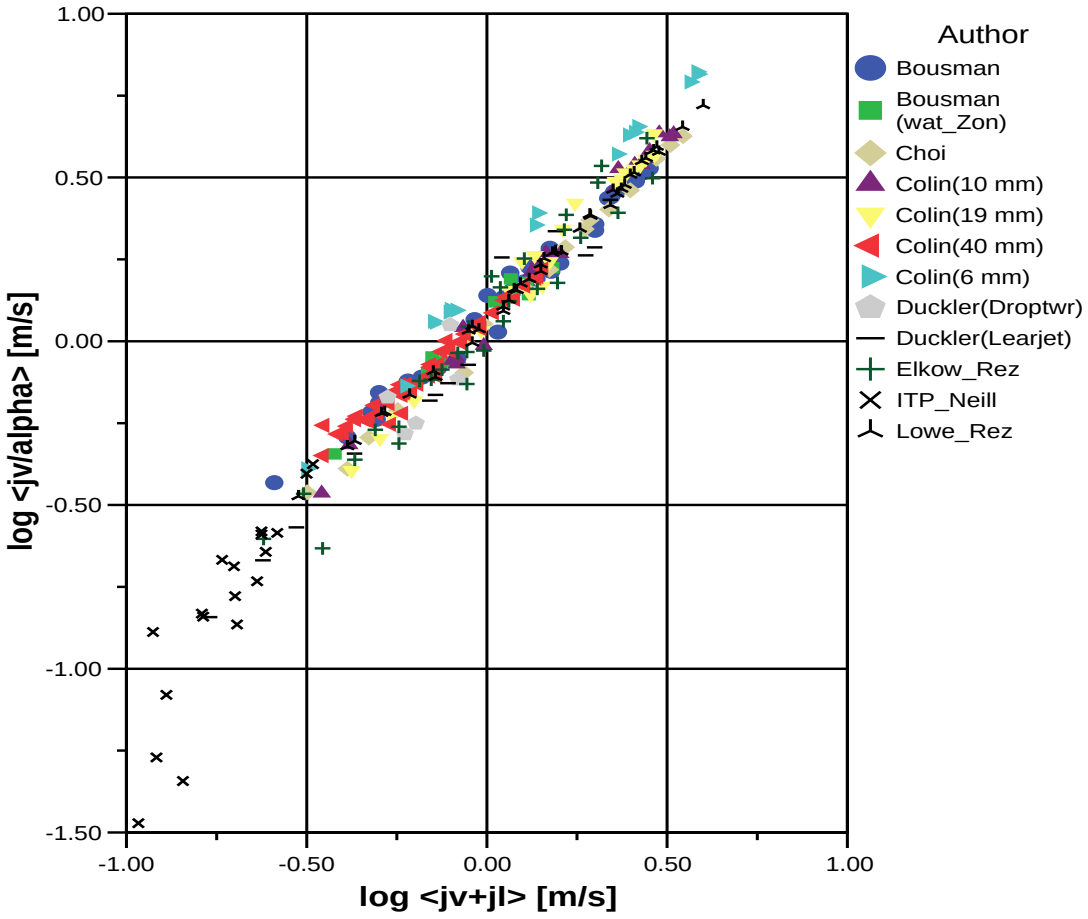

Figure 4.4 Transformed Slug Flow Plot for Various Researchers

A linear regression was performed on this data set and the results can be seen in Figure 4.5. The non-parametric tests were performed on these residuals to determine if the new data set met the axioms of a linear model. The data did not pass the Kruskal-Wallis test and had to be reduced further. This reduction was done based on looking at the mean ranks of each group and the distribution of residuals around zero. The first set

that was cut was Neill's data due to its negative distribution of residuals and the different slope this data displayed in Figure 4.5.

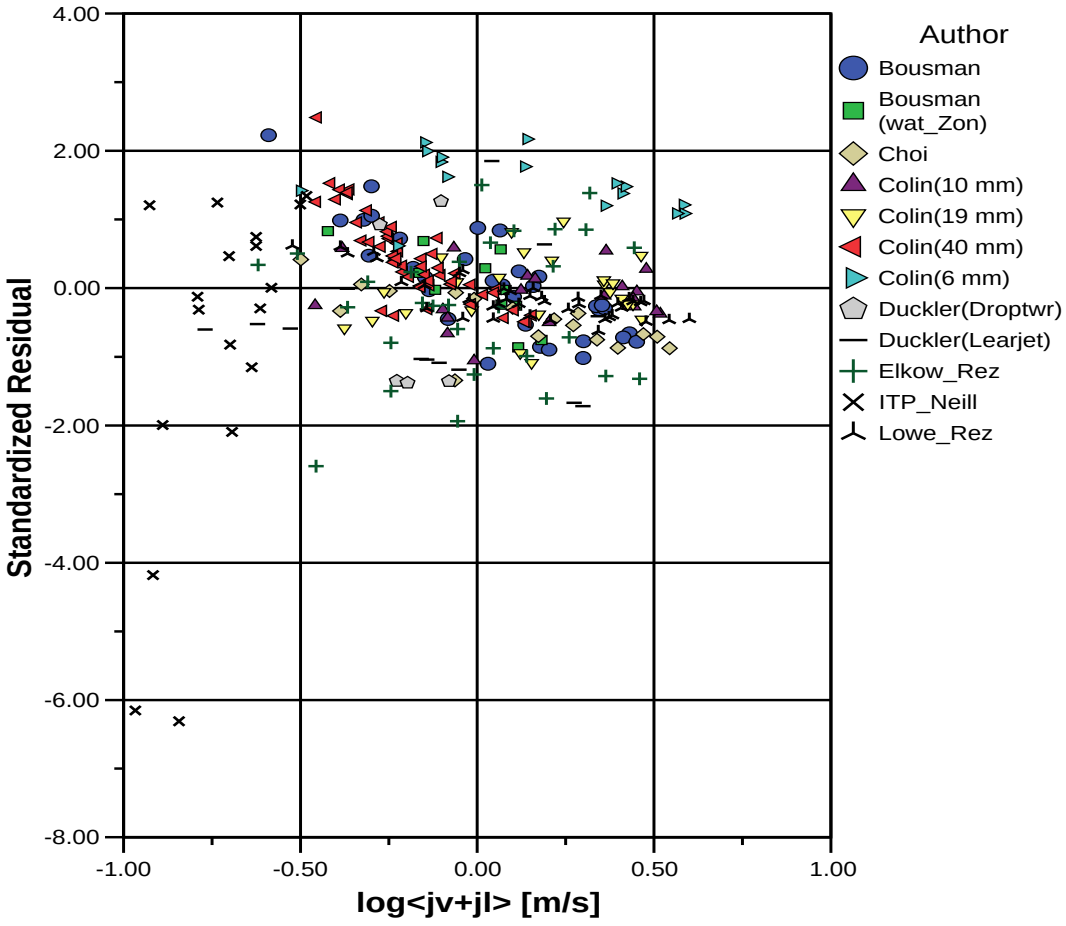

Figure 4.5 Standard Residuals vs. Log Mixture Velocity for Researchers

The removal of Neill's data returns the work flow back to the beginning. The linear regression of this new set was taken and their residuals were subsequently analyzed using non-parametric tests. The plot of these residuals is shown in Figure 4.6 and one can see that the distributions are close to or around zero for most of the data.

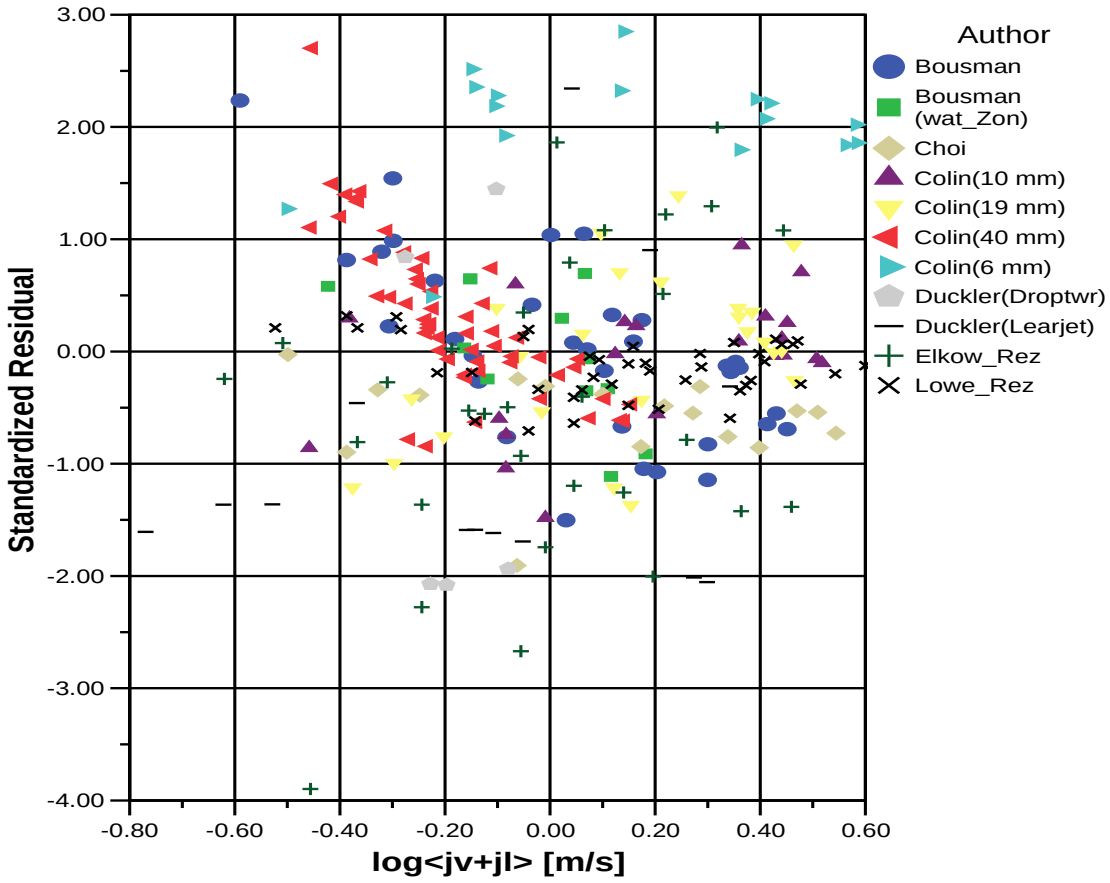

Figure 4.6 Standard Residuals vs. Log Mixture Velocity for Reduced Data Set

However, the data from Colin's 6 mm experiment visibly has a distribution around 2 instead of 0. There are two researchers with negative average residual values as well. Choi's data has a distribution of -0.5 and Duckler's Learjet data has a distribution of -1.5 instead of 0. This resulted in the removal of Choi's data, Colin's 6 mm data, and Duckler's Learjet data. Looking at the physical data of these points also raises concerns. It was noted in Choi (2002) that the values for the void fraction were larger than expected. Colin's 6 mm data was also suspect because of how the data

appears on the plot in Figure 4.3 and Figure 4.6. Colin's 6 mm group all are higher up the $log(j_g/\alpha)$ axis than any of the other points at those locations and do not fall on the linear line. The standard residuals for that group are also centered on two instead of zero. The final reduced data set, plotted in Figure 4.7, shows the transformed superficial gas velocity divided by the void fraction versus the transformed superficial mixture velocity. Looking at the figure one can see the line generated by the points is more compact and defined with the removal of the outlier data sets.

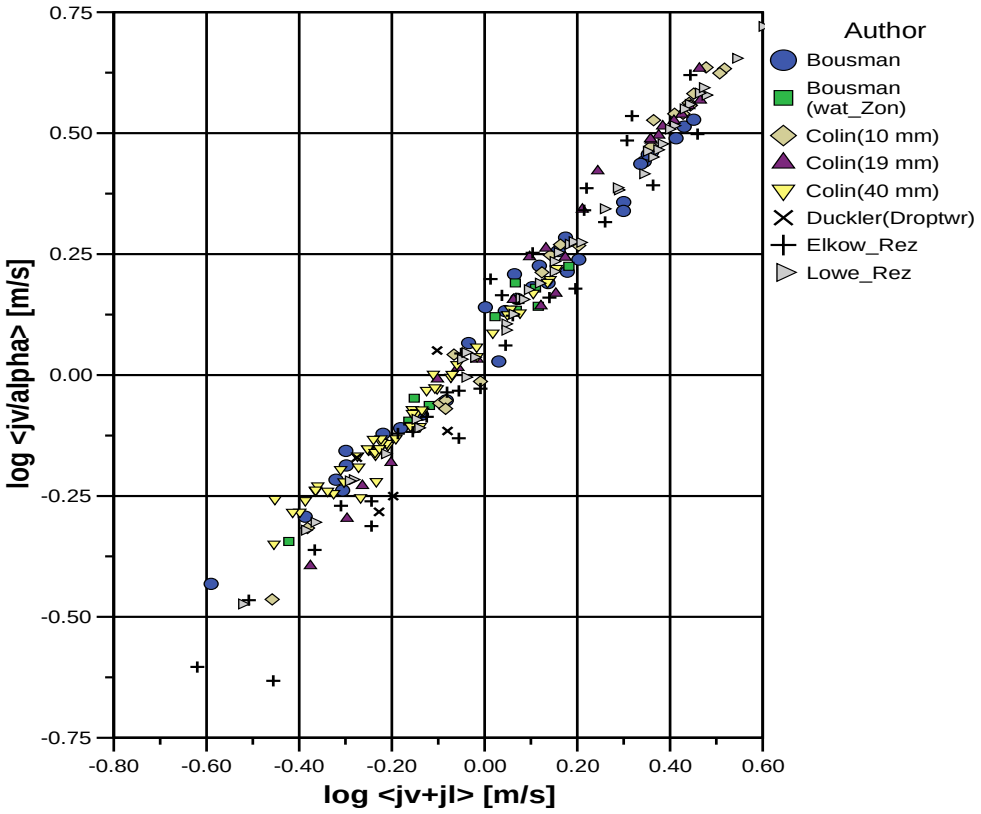

Figure 4.7 Transformed Slug Flow Plot for Final Reduced Data Set

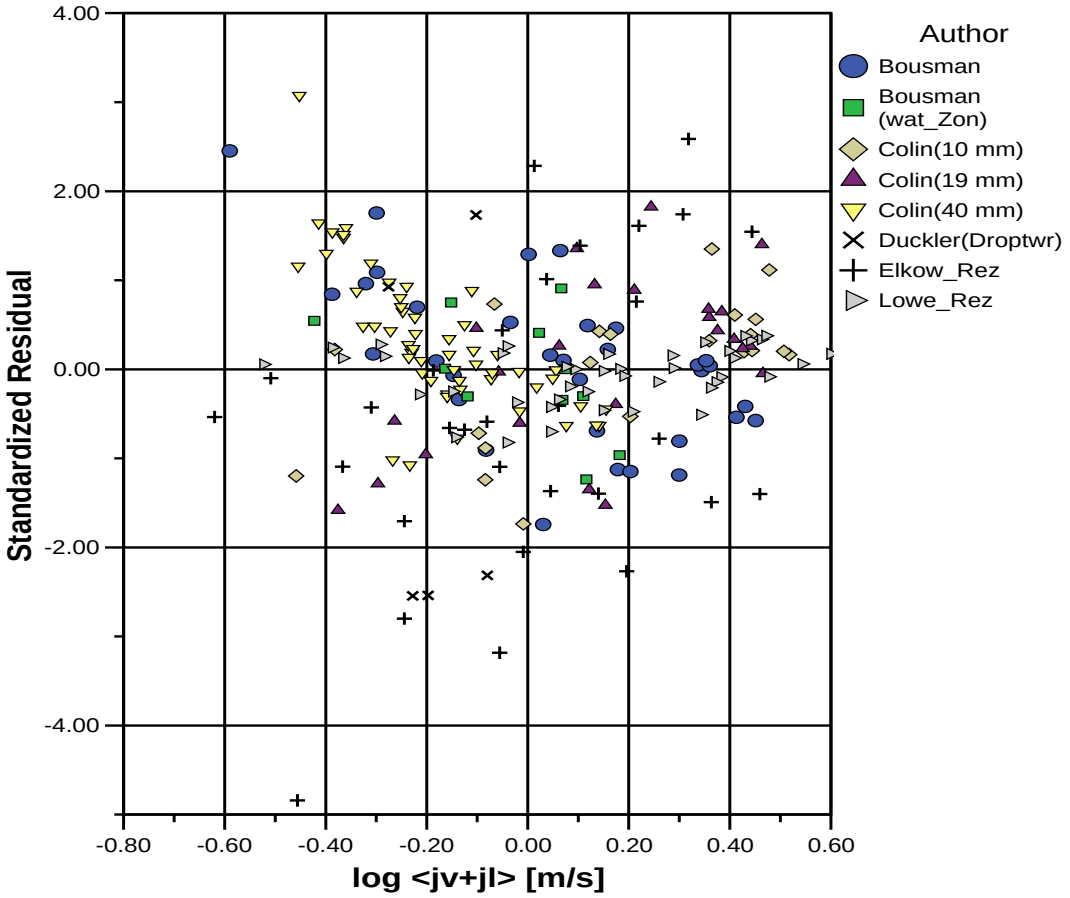

Figure 4.8 Standard Residual Plot for Final Reduced Data Set

The standard residuals plot in Figure 4.8 also shows a uniform distribution about zero for the residuals of the data, meaning that all of the points are distributed evenly about the regression line. With a usable data set generated from the transformation, the data set was then transformed from log values back to its original values. Figure 4.9 is a plot of the slug data points grouped by author, and shows the linear shape that the data takes. This allows for a statistical analysis of the non normalized data and can generate a non normalized distribution parameter and drift velocity.

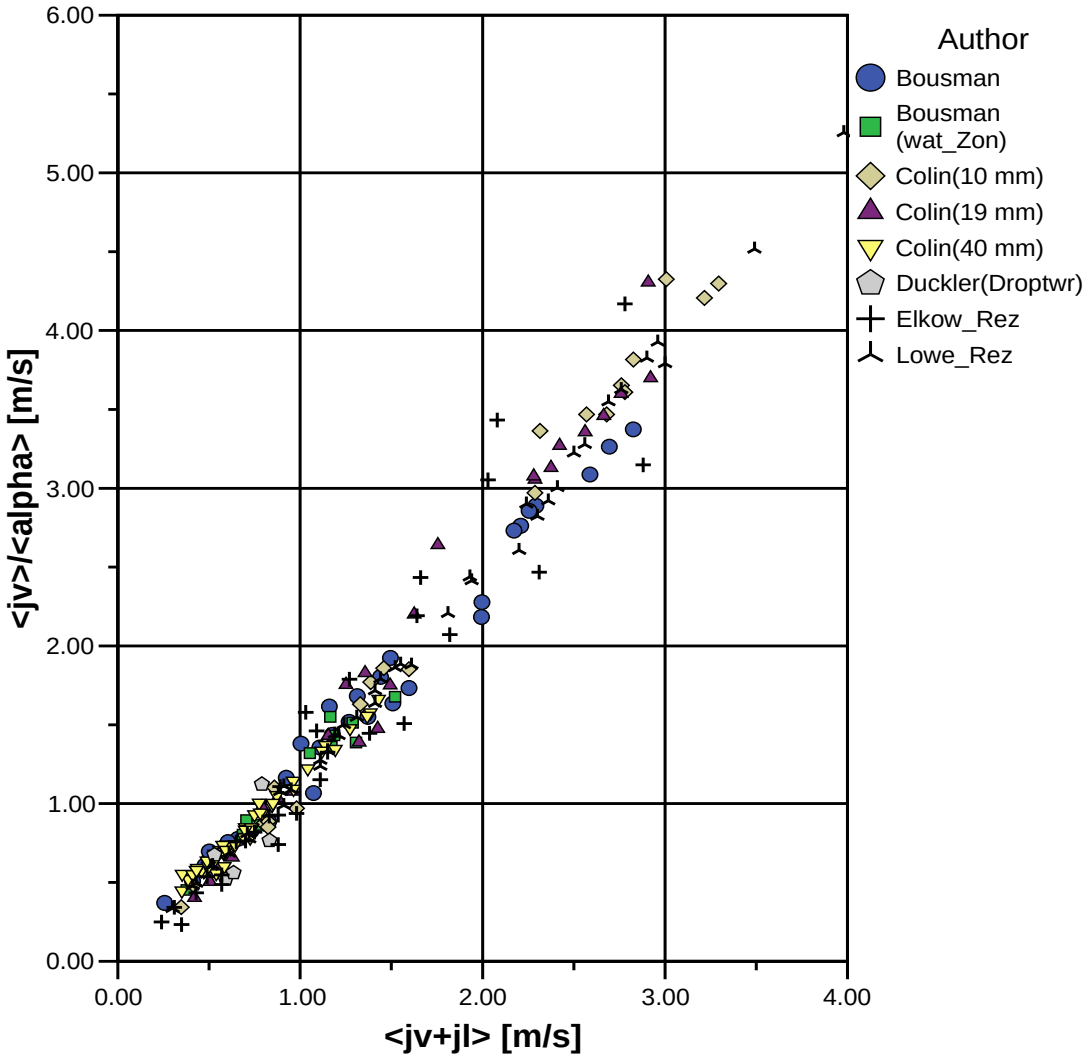

Figure 4.9 Reduced Slug Data Set

A regression was then preformed on the untransformed data which resulted in a distribution parameter of 1.336 ± 0.013 and a drift velocity of -0.126 ± 0.020. The plot in Figure 4.10 shows the distribution of the residuals around zero and their superficial mixture velocity. Figure 4.11 shows the Cook's distances for the data set. The largest Cook's distance is roughly equal to 0.15 meaning there are not any significant outliers in

the data set that could throw of the regression values. The non-parametric tests were performed on these residuals to make sure they align with the data and the results of those tests are catalogued in Table 4.1.

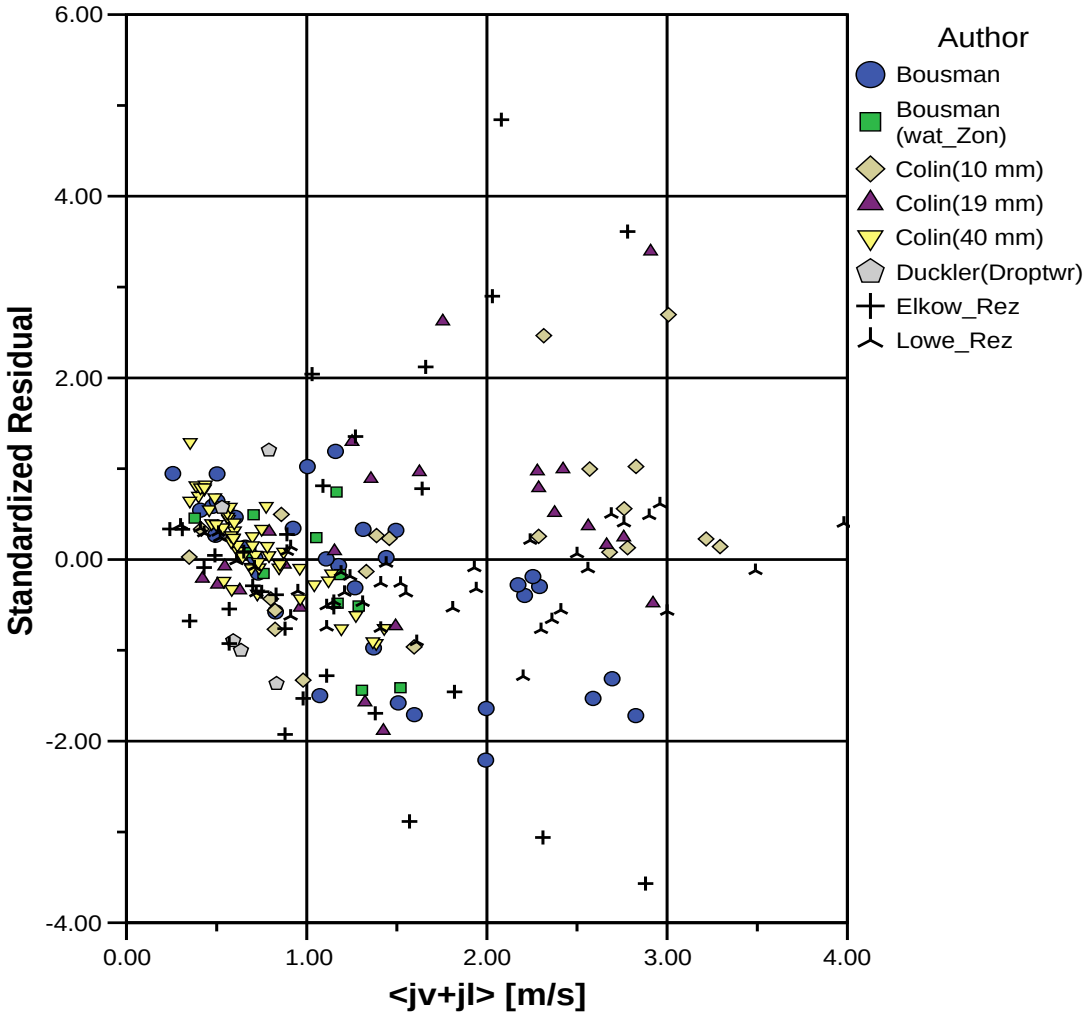

Figure 4.10 Standard Residuals of Reduced Data Set

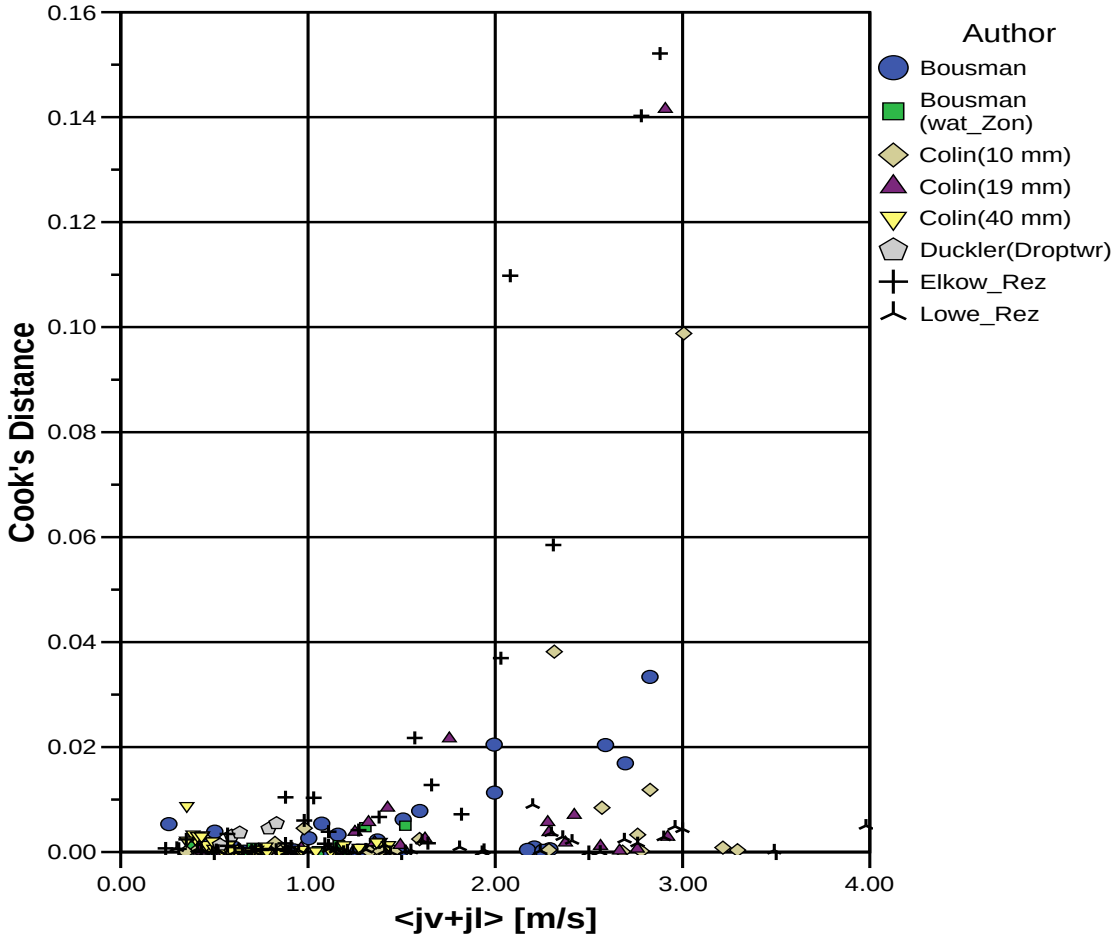

Figure 4.11 Cooks Distance for Reduced Data Set

The assumptions are tested and pass with a mean of 0.000 $^{+}/_{-}$ 0.191, an assumed p value of 0.05 was used unless otherwise stated. The distribution is normal based on the Kolmogorov-Smirnov tests shown in Table 4.1 and the histogram and quantile plot shown in Figures 4.12 and 4.13. Figure 4.13 represents the normality of the distribution in that the points are nearly a straight line with little variation towards the extreme end values. Table 4.1 also shows the breakdown of the data based on fluid type and author,

as well as the results of the non-parametric tests and the Bartlett's test. The total number of data points for each author and fluid type are broken down and the mean rank for each group are listed.

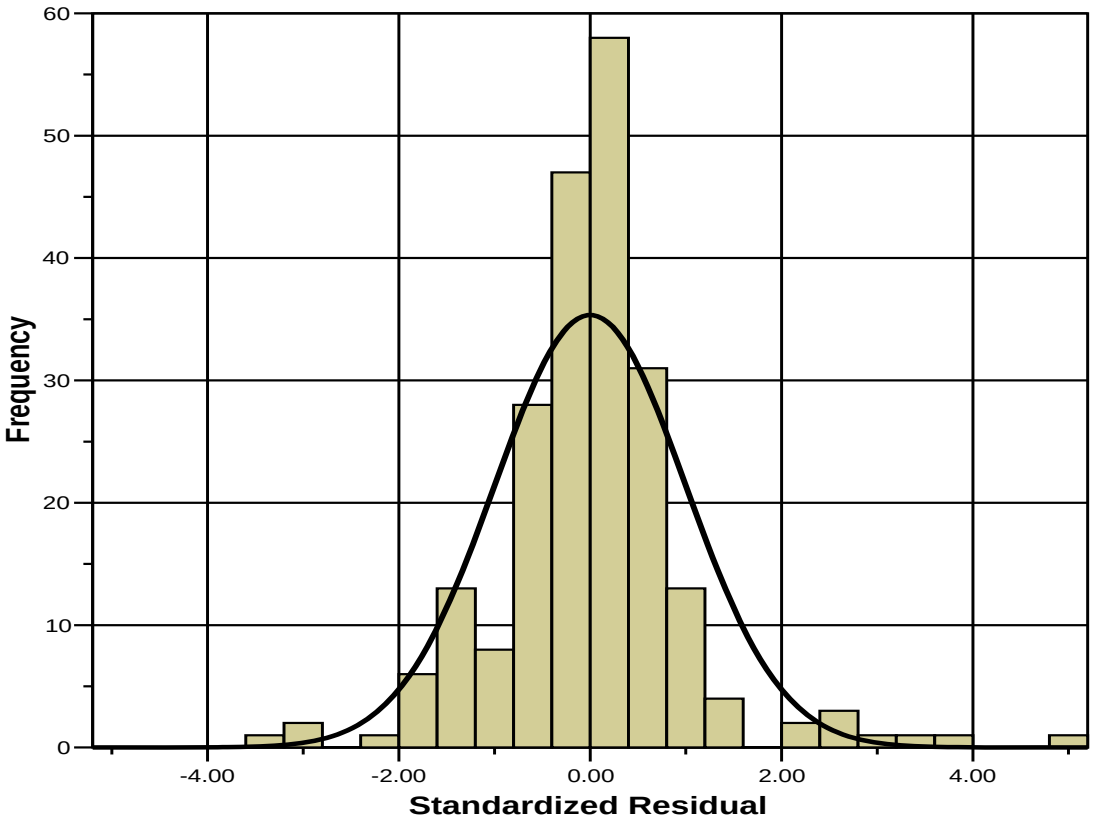

Figure 4.12 Histogram of Residuals Plotted with Normal Curve

Table 4.1 Results of Location Tests for Fluids and Authors

Standardized Residual

Fluid	n	Mean Rank	Sum of Ranks
Water/Air	210	111.6	23435
Water-Zonyl/Air	11	99.64	1096

Fluid Test Statistics

Mann-Whitney	1030
Wilcox	1096
Z	-0.605
Asymtotic Significance (2-tailed)	0.545
Kolmogorov-Smirnov	0.532
Asymptotic Significance (2-tailed)	0.94
Wald-Wolfowitz Runs - # of Runs	21
Z	-0.685
Asymptotic Significance (1-tailed)	0.255

Author	n	Mean Rank
Bousman	33	99.61
Bousman (wat_Zon)	11	99.64
Colin (19mm)	24	129.54
Colin (10mm)	21	126.24
Colin (40mm)	55	128.98
Dukler (droptower)	5	92.6
Elkow	30	98.03
Lowe	42	92.62

Author Test Statistics

Kruskal-Wallis Chi Square	14.074
df	7
Asymptotic Significance	0.05
Bartlett's Test of Sphericity Chi Square	4.811
df	1
Significance	0.028

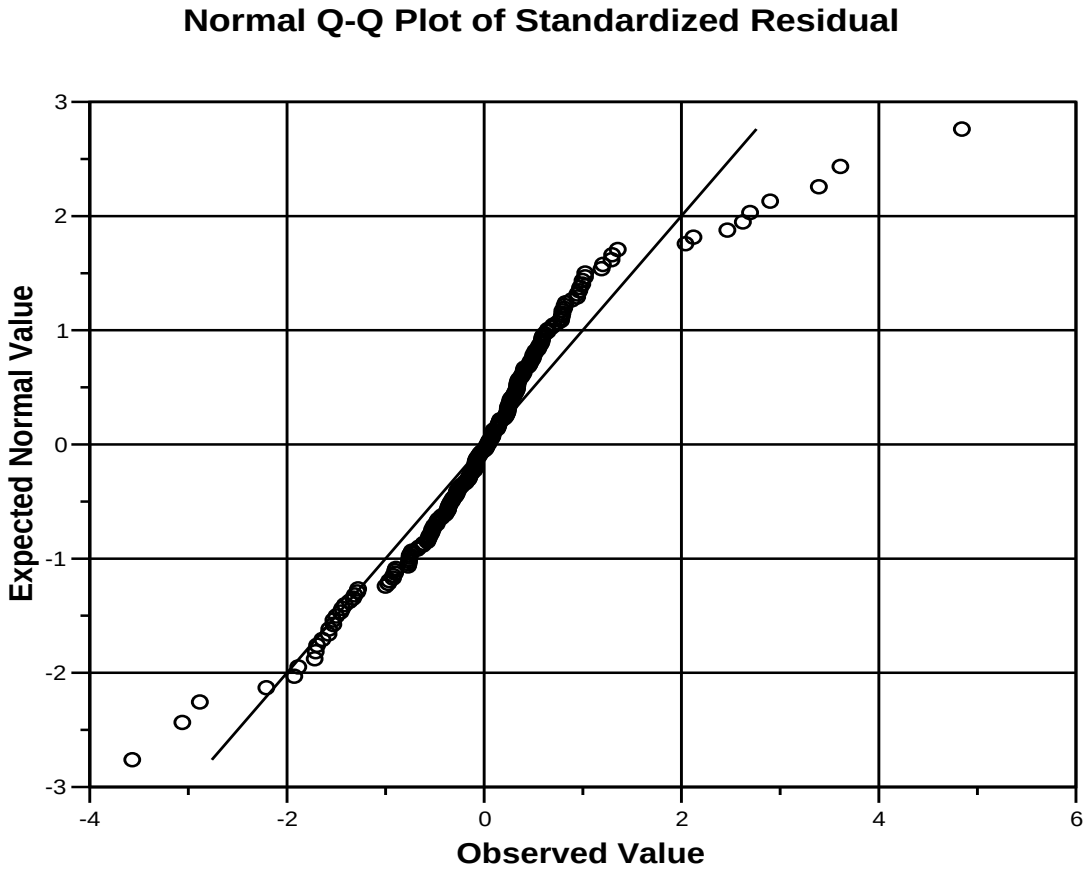

Figure 4.13 Normal Quantile Plot of Residuals

A similar approach is used for R12 and the Water-Glycerin mixture. The two fluids were combined in an attempt to make a second data set, however the resulting residuals failed the non-parametric statistical tests when comparing their means. This is significant in that individual analysis of the different fluid types resulted in a wide range of drift flux parameters. This combined with the statistical results when comparing the fluid types point towards the liquid properties having a large impact on the drift flux

parameters. Zonyl was added to the experiment resulting in a decrease in surface tension but does not impact the results of the statistical tests. However the density ratio of the working fluid seems to impact the results greatly and would mean that density ratio should be considered for future experiments. Therefore, each fluid is analyzed separately. The drift-flux parameters for each are shown below in Table 4.2 along with physical properties.

The drift-flux parameters for the reduced data set are not what would be expected by following the terrestrial drift flux model. If the terrestrial model held true, then one would expect to see results similar to terrestrial vertical upflow with drift flux parameters approximately equal to $C_o \approx 1.2$ and $u_{gj} \approx 0$ due to the absence of gravity. The microgravity aircraft produces microgravity conditions on the order of 10^{-3} m/s^2.Applying these gravity values to the empirical terrestrial vertical upflow equation, eq. (34), produces a drift velocity value on the order of 10^{-3} m/s. This value is well below the magnitude of the drift velocity observed in the data which is on the order of 10^{-1} m/s and enforces that the buoyancy forces have little impact on the microgravity drift velocity. An analysis of these values is performed in the next chapter as well as a physical interpretation of the results.

Table 4.2 Statistical Validated Drift Flux Parameters

Fluid	U_{gj}	C_0	□l ($^{kg}/_{m}3$)	□v ($^{kg}/_{m}3$)	□□(cP)	□.($^{dyne}/_{cm}$)
Water/air	-0.126 ± 0.020	1.336 ± 0.013	1000	~1	1	72
Water-Zonyl/Air					1	21
R12	-0.072 ± 0.022	1.448 ± 0.054	1320	34	23	10
Water-Glycerin/Air	0.054 ± 0.038	1.240 ± 0.024	~1130	~1	6	63

CHAPTER V

PHYSICAL INTERPRETATION OF THE DATA SET

5.1 INTRODUCTION

Applying the linear model to the raw data set has produced a statistically valid data set for water/air and water-zonyl/air mixtures. This section examines the physical interpretation of that data set as it applies to the drift flux model and provides calculations for the parameters in microgravity conditions. The values for the drift flux components from the linear model were $C_o = 1.336 \pm 0.013$ and $u_{gj} = -0.126 \pm 0.020$.

5.2 CALCULATION OF THE DISTRIBUTION PARAMETER

The data from the statistical analysis gave a distribution parameter, C_o, equal to 1.336. An inspection of the calculated value of C_o to the profile curves shown in Figure 2.1 appear to produce values of $m = 2$ and $n = 2$ for the velocity distribution and void distribution. The parabolic shape of the nose of the Taylor bubble show in the profiles of Figure 2.1 is due to the thicker liquid film in microgravity and has been documented in the works of Wheeler (1992) and Reinarts (1993).

Following the development of the distribution parameter from chapter 2, we can directly solve for the values of m and n and compare the corresponding C_o to the C_o determined statistically from the regression analysis. The first step of the C_o calculation is calculating values for j_c and r from Equations 16 and 19 respectively. These values then plug into Equation 14 to solve for m and Equation 15 to solve for n. Due to the lack of entrainment in microgravity two-phase flow it can be assumed $\acute{a}_w = 0$ and $\acute{a}_w/\acute{a}_c = 0$.

This comes from visual observation of microgravity slug flow and lack of bubbles entrained in the liquid film and slug as reported in Reinarts (1993).

Values for m and n for each data point were calculated using Equation 24 and Equation 29 respectively and the average of these numbers taken. Solving these two equations resulted in values of m and n equal to 2.261.

Solving Equation 31 for C_o in terms of the centreline gave a value equal to 1.335 which is very close to the value calculated statistically of 1.336 ± 0.013 to a confidence of 95% for the distribution parameter calculated from the linear model. This value makes physical sense due to the lack of gas entrainment observed in the liquid slugs and film thickness found in Reinarts (1993) for microgravity two-phase flow. The value of $Co = 1.336$ was calculated using a well developed model from the literature applying appropriate microgravity assumptions. This value is the same as value based on the statistically consistent analysis of experimental data.

5.3 CALCULATION OF THE DRIFT VELOCITY

The drift velocity poses a more difficult challenge because only empirical models exist and none of them have appropriate assumptions for microgravity. In the past, Equation 34 has been used setting the gravity term equal to 0, which results in a drift velocity equal to 0. However our statistically consistent analysis of the data produces a negative drift velocity and it would appear that the physics observed for terrestrial horizontal flow may be considered for microgravity conditions.

Other researchers have already discussed the conditions of a negative drift velocity in two-phase flow (Franca & Lahey 1992). As pointed out in the literature

review in chapter 1, this paper highlighted that the drift velocity, u_{gj}, is not normally zero for horizontal slug flows and that this assumption of a zero value was in part a misunderstanding of what the drift velocity represents. This is also the case for microgravity two-phase slug flow. The displacement experienced by the gas bubble and its expansion due to high pressure drop and the liquid velocity distribution in the slug can account for the negative drift velocity observed in microgravity. The displacement is supported by research into the bubble shape and film thickness performed by the ITP laboratory at Texas A&M University which shows the tip of the Taylor bubble having a well defined parabolic shape (Reinarts 1993). For the same superficial velocities, thicker liquid films will result in increased gas velocities due to the squeezing of the bubble by the film. This produces a much different liquid velocity profile between the film and the slug than is normally observed.

The work of O. Kvernvold et al. on the liquid velocity profile provides a basis for connecting the values obtained from the linear model to the physical process occurring in the pipe. As mentioned in chapter 1, the bubble moves through the test section it is forcing the liquid slug in front of it to move at an increased speed effecting the velocity distribution, which is exasperated in microgravity. This impacts the drift velocity which is a relationship of the relative velocities of the liquid and gas. The translational velocity results from Equation 11 were applied to the mixture velocity and used to calculate the drift velocity. The translational velocity was applied to Equation 11 by multiplying the mixture velocity by the coefficient from Equation 35 and subtracting the superficial gas velocity from this new value to give the adjusted liquid superficial velocity as shown in

Equation 41 below. Solving Equation 41 with the reduced data set resulted in a value for u_{gj} of -0.187.

$$u_{gj} = j_g - \alpha\left[j_g + \left(1.52j - j_g\right)\right] \tag{41}$$

This is smaller than the drift velocity value from the model, although it is still on the same order of magnitude. The variance in the two values can be attributed to multiple sources; the Kvernvold et al. experiment was for horizontal flow in terrestrial gravity conditions so buoyancy forces play a role in the way the liquid moves around the bubble. The film thickness and wall interfaces are also different between the two, with the bubbles from the Kvernvold et al. experiment travelling along the top wall of the pipe and bubbles in microgravity experiments traversing the centreline of the pipe with a liquid film between it and the pipe wall.

The relationships expressed in Equation 34 are for a bubble rising through a stagnant liquid, which is not the case in microgravity two-phase flow. Under microgravity two-phase flow conditions the liquid is being pulled along with the bubble through the pipe. In the terrestrial case all the relationships for drift velocity are for bubbles rising through a stagnant liquid. For microgravity this is not the case as the conditions are two-phase concurrent flow. Without buoyancy forces effecting microgravity two-phase flow, new dimensionless number parameters have to be selected. The capillary force was selected to replace buoyancy force as the dominant force in the development of the dimensionless numbers in Equation 15a, 15b, and 15c. These dimensionless numbers are the beginning steps of the model for determining an equation for the drift velocity in microgravity.

$$\pi_d = \frac{\rho_f v^2 D}{\sigma} \tag{42a}$$

$$\pi_e = \frac{\mu v}{\sigma} \tag{42b}$$

$$\pi_f = \frac{gD^2(\rho_f - \rho_g)}{\sigma} \tag{42c}$$

One potential model for drift velocity is a force balance of all the dimensionless numbers listed in Equation 32. Assuming that the sum of these forces is zero, the quadratic representation of this model is shown in Equation 43 and the resulting quadratic formula is Equation 44.

$$0 = \frac{\rho_f u_{gj}^2 D}{\sigma} + \frac{\mu u_{gj}}{\sigma} + \frac{gD^2 \Delta\rho}{\sigma} \tag{43}$$

$$u_{gj} = \frac{-\frac{\mu}{\sigma} \pm \sqrt{\left(\frac{\mu}{\sigma}\right)^2 - 4\left(\frac{\rho_f D}{\sigma}\right)\left(\frac{gD^2\Delta\rho}{\sigma}\right)}}{2\left(\frac{\rho_f D}{\sigma}\right)} \tag{44}$$

This equation shows that for a significantly small value of gravity, it is possible to have a negative drift velocity. Surface tension was chosen because of the influence these forces exert on the slug to annular transition. The surface tension acting on the nose of the Taylor bubble works against the annular transition. It is proposed that the surface tension at the bubble nose is essentially catching the gas flow. When gas inertial forces are greater than the surface tension forces the gas bridges the gap through the liquid slug to the tail of the elongated bubble creating annular flow (Reinarts 1993). The next step for this derivation is determining the film thickness of the liquid. However, certain characteristics differ between terrestrial and microgravity film thickness. First is the lack of entrainment between the liquid and gas that is common in terrestrial two-

phase flow and second is the generally thicker film thickness found in microgravity two-phase flow.

Figure 5.1 shows the prediction line and the 95% confidence interval plotted with the statistically consistent data set. The distribution of the data is showcased in Figure 5.1, with the majority of points falling below a superficial mixture velocity of 2. One observation drawn from Figure 5.1 is that improvements to the accuracy of the prediction line could be achieved be collecting more data with lower superficial velocities and reanalysing the data. This is discussed further in the conclusions in chapter 6.

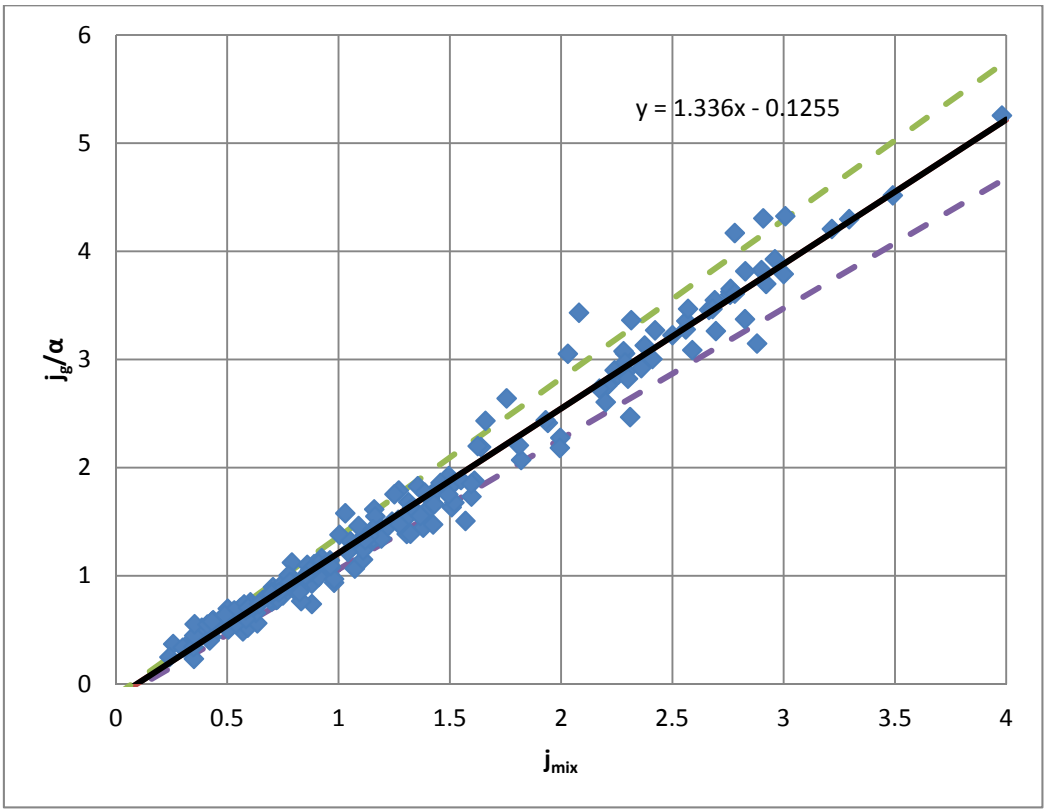

Figure 5.1 Prediction Line with 95% Confidence Intervals

Figure 5.2 shows a comparison between the newly developed prediction model of C_o = 1.336 and u_{gj} = -0.126 and the prediction model using the old assumptions of C_o = 1.2 and u_{gj} = 0 for the drift flux parameters. The figure also shows contour plots for both prediction models. The new prediction model provides a greater consistency in predicting void fraction values compared to the old model which varies both above and below expected values over the flow range. The new prediction model does have larger errors associated with very low mixture velocities however this can be attributed to difficulty achieving flow equilibrium at the low flow rates as well as potential bubbly-slug flow transitions.

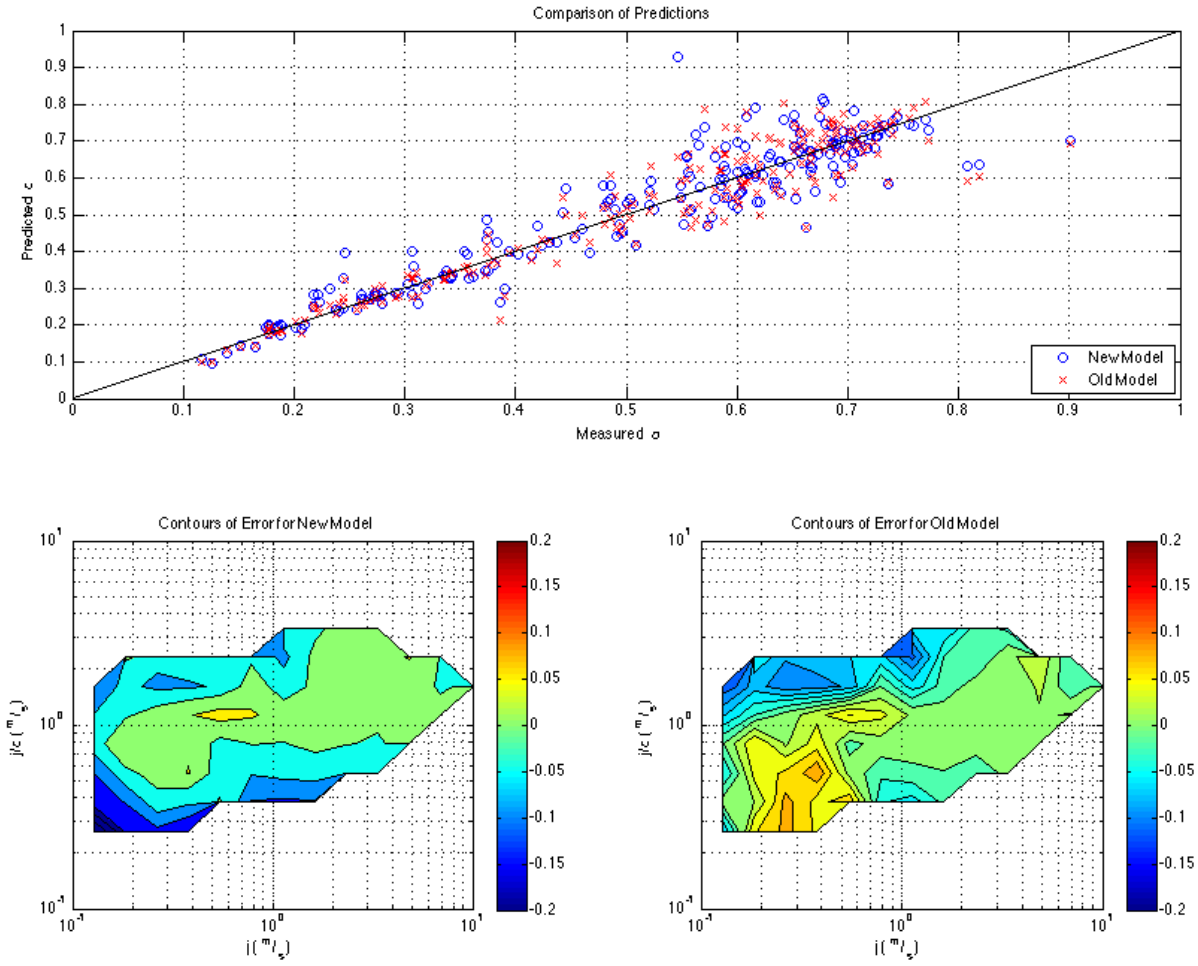

Figure 5.2 Error Comparison and Contours of New and Old Prediction Model

CHAPTER VI

CONCLUSIONS

6.1 REVIEW OF RESEARCH

The current knowledge of flow parameters for terrestrial two-phase flow was developed through experiments that collected hundreds to thousands of data points. However, the cost associated with microgravity testing make collecting such amounts of microgravity two-phase flow data difficult. Multiple researchers have attempted to calculate the microgravity drift flux model parameters by applying the methods initially developed by researchers such as Dumitrescu, Davies, and Taylor. However, these methods were developed with no consideration given to a microgravity environment. The purpose of this study was to develop a process by which results from multiple microgravity experiments can be compared on a similar medium and used to develop a larger viable data set than previously available and to reliably calculate a value for the void fraction from available data.

Slug flow data from 13 microgravity two-phase flow experiments was gathered for the purpose of developing a valid large scale microgravity slug flow data base. The analysis of this data was carried out using a combination of parametric and non-parametric statistical tests and the SPSS statistical software to produce a statistically consistent data set. The basis for these tests was to validate the four axioms of the linear model. The Kolmogorov-Smirov and Wald-Wolfowitz Runs tests were used to confirm the axiom that the residuals were independent. The Mann-Whitney U and the Kruskal Wallis tests were used to verify that the mean of the residuals was zero. The Bartlett test

was used to confirm the residuals variance was constant. The Q-Q plot and the histogram plot were used to verify the final axiom that the residuals followed a normal distribution. The final result was a data set consisting of 221 points of microgravity two-phase slug flow data from 8 different experiments.

Through validation of the four axioms of a linear model a data set was constructed of statistically consistent data from 8 different researchers. The drift flux parameters from this data set were a distribution parameter, C_o = 1.336 ± 0.013 and a drift velocity, u_{gj} = -0.126 ± 0.020. Observations of the other working fluids and their results suggest that density ratio of the working fluids have a large impact on the drift flux model and should be considered in experiment construction. The physical interpretation of the drift flux parameters for the valid data set was determined by examining the development of the drift flux model, the distribution parameter, and the drift velocity. Calculated values of the distribution parameter and drift velocity matched well with the results of the linear model of the data set. The developed method for calculating the drift velocity explains the negative values observed in microgravity drift velocity. Based on the validation of the data, the drift flux parameters can be used to calculate a void fraction for air and water two-phase flow systems using the flow rates of the system.

6.2 FUTURE WORK

As manned space exploration expands and scales up, so must the systems involved in this exploration expand and scale up. The problem with applying current terrestrial models is that for very small scale systems the deviations of the model from

experimental data are difficult to detect, but as systems are scaled up and larger flow rates and pipes are required these deviations become more apparent and knowledge of what is transpiring in the system becomes more uncertain. The process proposed in this thesis not only analyses the drift flux parameters but also presents an approach to data validation that can be used to predict values of larger two-phase flow systems. This process can be performed as more microgravity two-phase flow data becomes available in a continuous effort to increase the amount of statistically vetted data. Targeted experiments could be performed to increase the amount of data at higher mixture flow rates could lead to a more even distribution of the data and decrease the error range observed in higher mixture flow rates. Increasing the overall volume of data in turn will lead to more accurate representation of the Drift Flux model. Further tests on other flow regimes, e.g. bubbly and annular flow would provide a basis for moving away from visual identification of flow regimes as well as broaden the methods outlined in this thesis.

REFERENCES

Bousman, W.S., 1994. Studies of Two-Phase Gas-Liquid Flow in Microgravity. Ph.D. Dissertation, University of Houston, Houston, TX.

Bousman, W.S., McQuillen, J.B., Witte, L.C., 1996. Gas-Liquid Flow Patterns in Microgravity: Effects of Tube Diameter, Liquid Viscosity and Surface Tension. Int. J. Multiphase Flow Vol. 22, No. 6, pp. 1035-1053.

Braisted, J.D., 2004. Drift-Flux Analysis of Two-Phase Flow in Microgravity. M.S. Thesis, Texas A&M University, College Station, TX.

Chang, J.H., 1997. Statistical Comparison of Two-Phase Flow, Void Fraction Fluctuations in a Microgravity Environment. M.S. Thesis, Texas A&M University, College Station, TX.

Crowley, C.J., Chen, W.B., 2001. Scaling of Multiphase Flow Regimes and Interfacial Behaviour at Microgravity. NASA Glenn Research Center, Contract NAS3-98113 Cleveland, OH.

Choi, B., Fuji, T., Asano, H., Sugimoto, K., 2002. A Study of Gas-Liquid Two-Phase Flow in a Horizontal Tube Under Microgravity. Ann. N.Y. Acad. Sci. 974, 316-327.

Clarke, N.N., Rezkallah, K.S., 2001. A Study of Drift Velocity in Bubbly Two-Phase Flow Under Microgravity Conditions. Int. J. Multiphase Flow Vol. 27, No. 9, pp. 1533-1554.

Colin, C., Fabre, J., Dukler, A.E., 1991. Gas-Liquid Flow at Microgravity Conditions-1: Dispersed bubble and Slug Flow. Int. J. of Multiphase Flow Vol. 17, No. 8, pp. 533-544.

Colin, C., Fabre, J., McQuillen, J., 1996. Bubble and Slug Flow at Microgravity Conditions: State of Knowledge and Open Questions. Chem. Eng. Comm., Vols. 141 142, pp. 155-173.

Collier, J.G., Thome, J.R., 2001. Convective Boiling and Condensation Third Edition, Oxford Science Publications, Oxford, UK.

Davies, R.M., Taylor, G., 1950. The Mechanics of Large Bubbles Rising through Extended Liquids and Through Liquids in Tubes. Proc. R. Soc. Lond. A, 375-390.

Duckler, A.E., Fabre, J.A., McQuillen, J.B., Vernon, R., 1988. Gas-Liquid Flow at Microgravity Conditions: Flow Patterns and Their Transitions. Int. J. of Multiphase Flow Vol. 14, No. 4, pp. 389-400.

Dumitrescu, D.T., 1943. Stromung and Einer Luftbluse in Senkrechten rohr. Z. Angew. Math. Mech. 23, 139-149.

Elkow, K.J., Rezkallah, K.S., 1997. Void Fraction Measurements in Gas-Liquid Flows Under 1-g and μ-g Conditions Using Capacitance Sensors. Int. J. of Multiphase Flow Vol. 23, No. 5, pp. 815-829.

França, F., Lahey Jr., R.T., 1992. The use of drift-flux techniques for the analysis of horizontal two-phase flows. Int. J. Multiphase Flow Vol. 18, No. 6, pp. 787-801.

Kvernvold, O., Vindøy, V., Søntvedt, T., Saasen, A., Selmer-Olsen, S., 1984. Velocity Distribution in Horizontal Slug Flow. Int. J. Multiphase Flow Vol. 10, No. 4, pp. 441-457.

Lowe, D.C., Rezkallah, K.S., 1999. Flow Regime Identification in Microgravity Two-Phase Flows Using Void Fraction Signals. Int. J. Multiphase Flow Vol. 25, No. 4, pp. 433-457

Nguyen, N.T., 2009. Analytical and Experimental Study of Annular Two-Phase Flow Friction Pressure Drop Under Microgravity. M.S. Thesis, Texas A&M University, College Station, TX.

Nicklin, D.J., Wilkes, J.O., Davidson, J.F. 1962. Two-Phase Flow in Vertical Tubes. Trans. Instn. Chem. Engrs. 40, 61-68

Reinarts, T.R., 1993. Adiabatic Two-Phase Flow Regime Data and Modeling for Zero and Reduced (Horizontal Flow) Acceleration Fields. Ph.D. Dissertation, Texas A&M University, College Station, TX.

Shephard, A.M., 2009. Microgravity Flow Regime Transition Modelling. M.S. Thesis, Texas A&M University, College Station, TX.

Valota, L., 2004. Microgravity Flow Pattern Identification Using Void Fraction Signals. M.S. Thesis, Texas A&M University, College Station, TX.

Wallis, G.B., 1969. One-Dimensional Two-Phase Flow. McGraw-Hill Book Company, New York, NY.

Wheeler, M., 1992. An Experimental and Analytical Study of Annular Two-Phase Flow Friction Pressure Drop in a Reduced Acceleration Field. M.S. Thesis, Texas A&M University, College Station, TX.

Zhao, J.F., Hu, W.R., 2000. Slug to Annular Flow Transition of Microgravity Two-Phase Flow. Int. J. Multiphase Flow Vol. 26, No. 4, pp. 1295-1304

Zuber, N., Findlay, J.A., 1965. Average Volumetric Concentration in Two-Phase Flow Systems. J. Heat Transfer 87, 453-468.